NASA TECHNICAL REPORT

NASA TR R-377

NASA TR R-377

PHASE-LOCK DEMODULATION OF A PM SIGNAL CONTAMINATED WITH INCIDENTAL AM

by George B. Robinson

Goddard Space Flight Center
Greenbelt, Md. 20771

NATIONAL AERONAUTICS AND SPACE ADMINISTRATION • WASHINGTON, D. C. • FEBRUARY 1972

1. Report No. NASA TR R-377	2. Government Accession No.	3. Recipient's Catalog No.
4. Title and Subtitle Phase-Lock Demodulation of a PM Signal Contaminated With Incidental AM		5. Report Date February 1972 6. Performing Organization Code
7. Author(s) George B. Robinson		8. Performing Organization Report No. G-1032
9. Performing Organization Name and Address Goddard Space Flight Center Greenbelt, Maryland 20771		10. Work Unit No. 11. Contract or Grant No. 13. Type of Report and Period Covered Technical Report
12. Sponsoring Agency Name and Address National Aeronautics and Space Administration Washington, D.C. 20546		14. Sponsoring Agency Code

15. Supplementary Notes

16. Abstract

Signals from phase-modulated satellite transmitters usually exhibit some degree of incidental amplitude modulation (AM). This report analyzes the effects of incidental AM when this type of signal is demodulated by a phase-lock receiver which does not employ a limiter preceding the loop phase detector. The presence of incidental AM causes a reduction in the receiver output signal-to-noise (S/N) ratio. The tolerable level of AM decreases in proportion to the phase modulation (PM) index β. For a square-wave modulating signal, a 1 dB reduction results at the receiver PM channel output when $\beta = 1$ radian and the percentage of AM = 23, $\beta = 1.2$ radians and the percentage of AM = 16, or $\beta = 1.5$ radians and the percentage of AM = 4. Although only the PM channel of the receiver is used ordinarily, utilizing both the AM and PM channel by summing offers an improvement in S/N relative to the S/N ratio of the PM channel if the percentage of incidental AM is greater than fifteen.

17. Key Words Suggested by Author	18. Distribution Statement
Phase Modulation Incidental AM Phase-Lock Demodulation	Unclassified–Unlimited

19. Security Classif. (of this report)	20. Security Classif. (of this page)	21. No. of Pages	22. Price
Unclassified	Unclassified	55	3.00

*For sale by the National Technical Information Service, Springfield, Virginia 22151

SUMMARY

This report analyzes the effects of incidental amplitude modulation (AM) on the demodulation channel output of a phase-lock receiver when the input signal is a square-wave phase-modulated carrier which also contains superimposed synchronous AM. This analysis is limited to receivers which do not employ a limiter preceding the loop phase detector. The analysis is of practical interest because some degree of incidental AM usually occurs in transmitters, and the use of third-order loop receivers which do not employ a limiter is common in ground stations.

The analysis shows that the effect of synchronous AM depends upon its phase relative to the impressed phase modulation (PM). In satellite transmitters, AM is most likely to occur in phase coincidence or in phase opposition.

In-phase AM or AM in phase opposition causes signal suppression and a consequent reduction in the signal-to-noise (S/N) ratio at the receiver PM channel demodulation output. The tolerable level of AM decreases with the degree of PM normally present. If the PM index β is normally 1 radian, 23 percent AM will cause a reduction of 1 dB; if $\beta = 1.2$ radians, 16 percent AM will cause a 1 dB reduction; if $\beta = 1.5$ radians, 4 percent AM will cause a 1 dB reduction.

Although only the PM channel is normally utilized, the analysis shows that summing both the PM and AM channels of the receiver will improve the S/N ratio for ranges of AM greater than 15 percent.

In-phase AM or AM in phase opposition alters the balance of power between the carrier and modulation components of the signal. Relative to a normal PM signal, incidental AM increases the carrier power, reduces the quadrature modulation power, and produces in-phase modulation power; in-phase modulation power is totally absent in normal square-wave PM.

The analysis also considers AM in quadrature with the impressed PM. This type of AM can be detected from its spectrum because it causes the normally symmetrical PM spectrum to become asymmetrical. The principal effect of this type of AM is the generation of a double-frequency distortion term.

CONTENTS

PHASE-LOCK DEMODULATION OF A PM SIGNAL CONTAMINATED WITH INCIDENTAL AM

by
George B. Robinson
Goddard Space Flight Center

CHAPTER 1

INTRODUCTION

The use of a phase-modulated carrier as a means of transmitting information from satellites has become rather common in recent years. Modulation of this type is produced by a variable phase-shift network incorporated in the transmitter. Ideally, such a network should produce a shift of the carrier in direct proportion to the amplitude of the modulating signal without simultaneously changing the amplitude of the carrier. In practice, there are a number of difficulties associated with the elimination of incidental amplitude modulation (AM). The phase modulator is one of the more complex networks incorporated in the transmitter. One type of circuit employed is a bridge T with varactor diodes as the variable reactance elements (Reference 1). Experience has shown that a critical requirement of this network is the exact termination in its characteristic impedance. Improper termination is a prime cause of incidental AM. A phase-modulated signal containing incidental AM cannot be optimally demodulated by a phase-lock receiver. This paper shows that when incidental AM is present in quadrature with the impressed phase modulation (PM), the receiver output will contain distortion terms. If incidental AM is in phase or in phase opposition relative to the impressed PM, the receiver output will experience suppression with a consequent reduction in the output signal-to-noise (S/N) power ratio. Incidental AM in phase or in phase opposition is considered most likely to occur in a satellite transmitter. Since little information has appeared in the literature, it is the intent of this work to provide a quantitative guide on the percentage of incidental AM that is tolerable in terms of the resultant distortion, or the reduction in the S/N ratio. The report will be restricted to square-wave modulation and will consider demodulation by a receiver which does not employ a limiter preceding the loop phase detector.

The report is divided into two sections. Case I is concerned with incidental AM in phase quadrature with the impressed PM. In this section, the spectrum of the signal is derived and compared with the spectrum of a normal PM signal not containing incidental AM. Then, the receiver output is derived

for a fixed PM index and a variable AM index. This expression permits an evaluation of the tolerable level of incidental AM in terms of the resultant distortion.

Case II is concerned with in-phase incidental AM and derives the spectrum and the receiver output; then, the output S/N ratio of the receiver is calculated. This latter relationship permits an evaluation of tolerable levels of incidental AM in terms of the reduction in the S/N ratio. Measurements to confirm the predicted receiver outputs are shown. Measurements were made with an Electrac Model-215 phase-lock demodulator, which is currently in use at the GSFC Space Tracking and Data Acquisition Network facility. Case II closes with a derivation of the carrier in-phase and quadrature power division characteristic of a square-wave PM signal when in-phase incidental AM is present.

CHAPTER 2

FORMULATION OF PROBLEM

An improperly terminated phase modulator of the type described in Reference 1 will cause the amplitude of the transmitter output to change simultaneously with the transmitter carrier phase shift. As an example, consider the measurements shown in Part A of Figure 1. These data show the output phase shift of a typical transmitter versus the dc input to the transmitter modulator. (The phase shift is measured relative to the transmitter crystal oscillator, as shown in Part B of Figure 1.) This plot, which is labeled Curve 1, establishes the PM characteristics of the transmitter. Curve 2 shows the output amplitude variation, which occurs synchronously because the phase modulator is improperly terminated. For actual transmitter operation, a dc bias is selected, and the modulation signal is superimposed on the bias. An expression for the phase shift produced by this particular transmitter can be derived as follows.

Choose a dc bias of 8 volts and erect a vertical line at the bias point. The vertical line will intersect the phase-shift curve (Curve 1). The static phase shift corresponding to this intersection is 2.51 radians, read on the scale on the right. If a signal $S(t)$ is superimposed on the bias, the resulting PM is $K_1 S(t)$, where K_1 is the slope of Curve 1 in radians per volt. Then, the output of the transmitter can be written as amplitude $\times \cos [\omega_c t + 2.51 + 2\theta_i + K_1 S(t)]$, where ω_c is the carrier frequency and θ_i is the initial phase angle of the transmitter crystal oscillator. The phase angle is included because the phase-shift curve was measured with the transmitter crystal oscillator as the reference, through an external doubler, as in Part B of Figure 1. The amplitude variation produced by the signal is obtained in a similar manner from Curve 2. The static output of the transmitter, determined from the intersection of the vertical bias line on Curve 2, is 0.533 volts peak from the scale on the left. The amplitude variation from a signal $S(t)$ is $-K_2 S(t)$, where K_2 is the slope of Curve 2 in volts per volt. The transmitter output amplitude, consequently, is $0.533 - K_2 S(t)$. The desired signal expression is $0.533 \times [1 - K_2 S(t)/0.533] \cos [\omega_c t + 2.51 + 2\theta_i + K_1 S(t)]$. Finally, if the signal $S(t)$ is symmetrical about the time axis and periodic with a peak amplitude E_{pk}, then let $S(t) = E_{pk} e(t)$, where $e(t)$ is expressed as a fraction of E_{pk}. The transmitter output, in terms of the modulation parameters β and M, is $E[1 - Me(t)] \cos [\omega_c t + \beta e(t)]$. When $E = 0.533$, $K_2 E_{pk}/0.533 = M$ [the AM modulation index (restricted to a value no greater than one)] and $K_1 E_{pk} = \beta$ (the peak PM index in radians). In the above signal expression, the total initial phase angle $2.51 + 2\theta_i$ has been ignored, since it does not affect the reception of the signal after lock has been established in the receiver. The expression as written describes a PM signal characterized by superimposed AM which is in phase opposition to the PM content of the signal, i.e., the AM term $Me(t)$ is preceded by a minus sign, while the term accounting for PM, $\beta e(t)$, is preceded by a positive sign. That the transmitter would produce AM in phase opposition can not be determined from the plots shown in Figure 1 since they are essentially static plots which do not

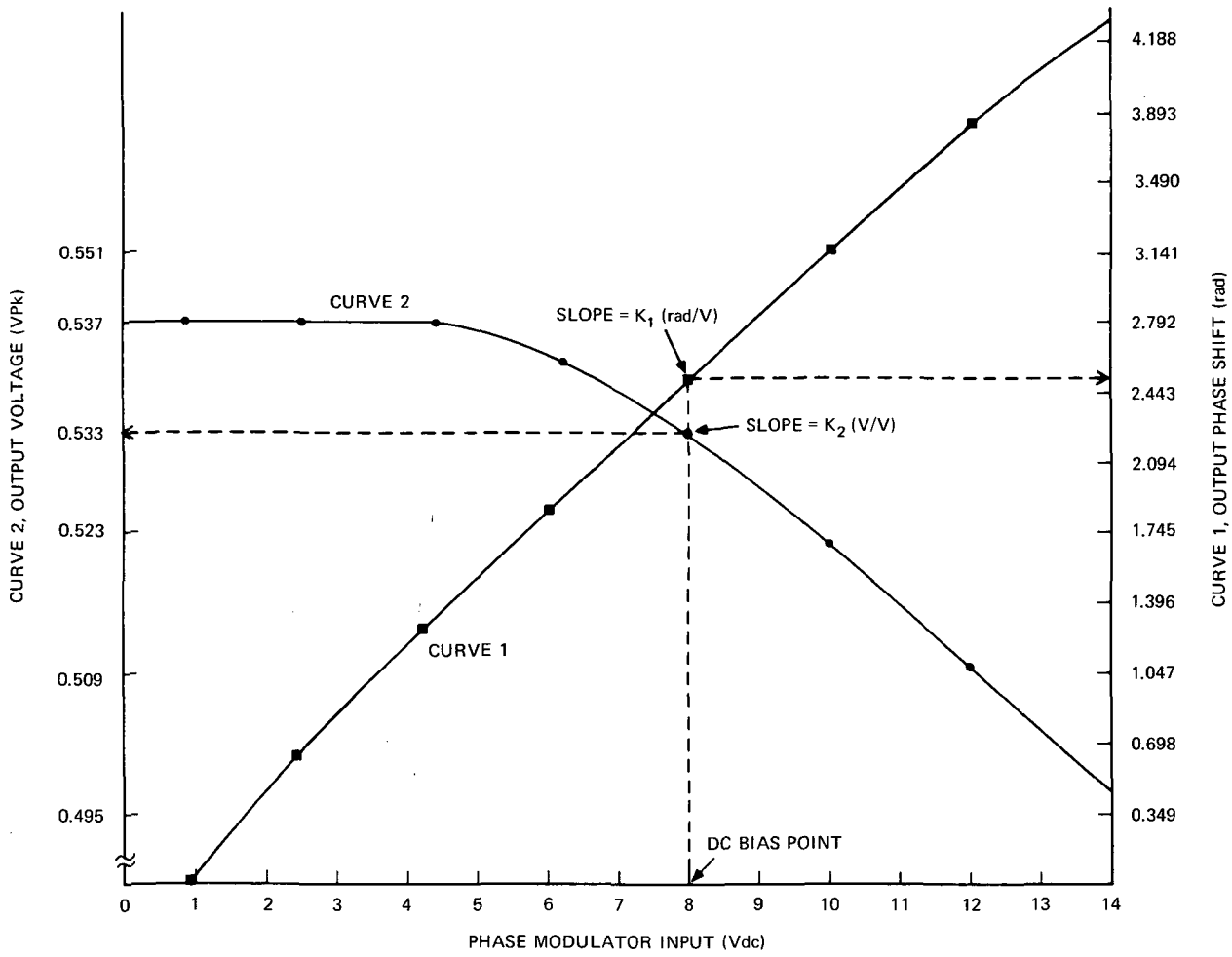

(A) Transmitter output amplitude (Curve 2) and phase shift (Curve 1) versus dc input to modulator.

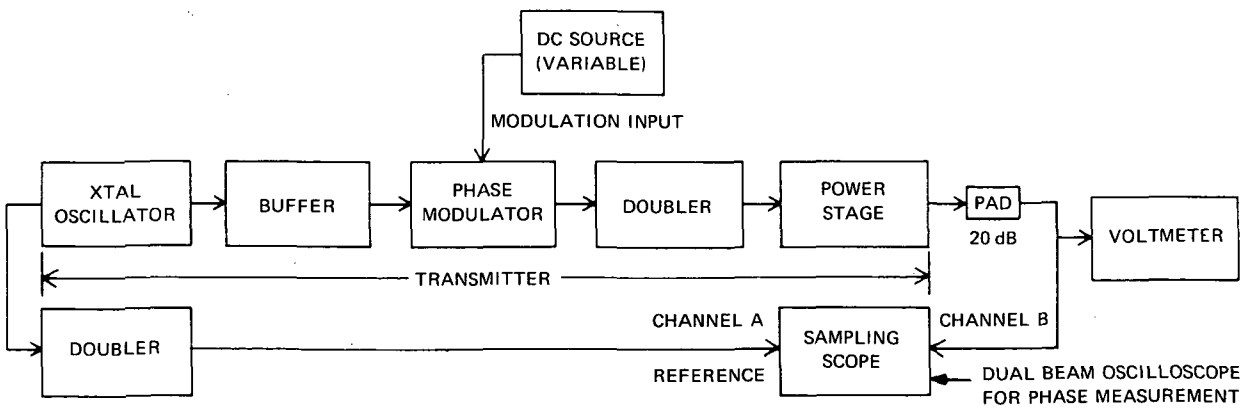

(B) Method of measurement.

Figure 1—Transmitter characteristics.

involve the frequency components making up $e(t)$. However, it will be shown that the phase ambiguity can be resolved from the signal spectrum and tests with the receiver. For the particular transmitter whose characteristics are shown in Part B of Figure 1, the superimposed AM is in phase opposition for both square- and sine-wave modulating signals with fundamental frequencies as high as 10 Hz. While it is not possible to say with certainty that this phase relationship would result at very high modulating frequencies, nevertheless, it is considered most probable, and the bulk of the report (Case II) will be devoted to this type of signal. To provide additional background information, square-wave modulation in quadrature will be treated briefly in Case I.

The use of a transmitter as a signal source for the study of incidental AM is not feasible because the percentage of AM relative to the degree of PM is fixed. A suitable system for this study is shown in Figure 2. In this test set-up, the modulating signal $S(t)$ obtained from a single source is applied simultaneously through attenuators to separate phase and amplitude modulators in tandem; the attenuators allow the degree of PM and AM to be adjusted independently. In this particular system, the signal carrier source and the phase modulator are combined in a single unit which drives a separate amplitude modulator. The output of the AM modulator is a phase-modulated signal with synchronous AM which simulates the transmitter output. This signal is, in turn, fed to a Model-215 phase-lock demodulator and to a spectrum analyzer at the demodulator input. Then, the demodulator outputs are measured with an oscilloscope and low-frequency spectrum analyzer. With this system, the input and output spectra of the receiver can be determined as functions of the AM and PM indexes M and β.

The square-wave source for the modulating signal is taken from a variable phase function generator (Figure 2) which provides a reference output and a separate variable phase output. The phase modulator is driven from the reference phase output, and the amplitude modulator is provided with a

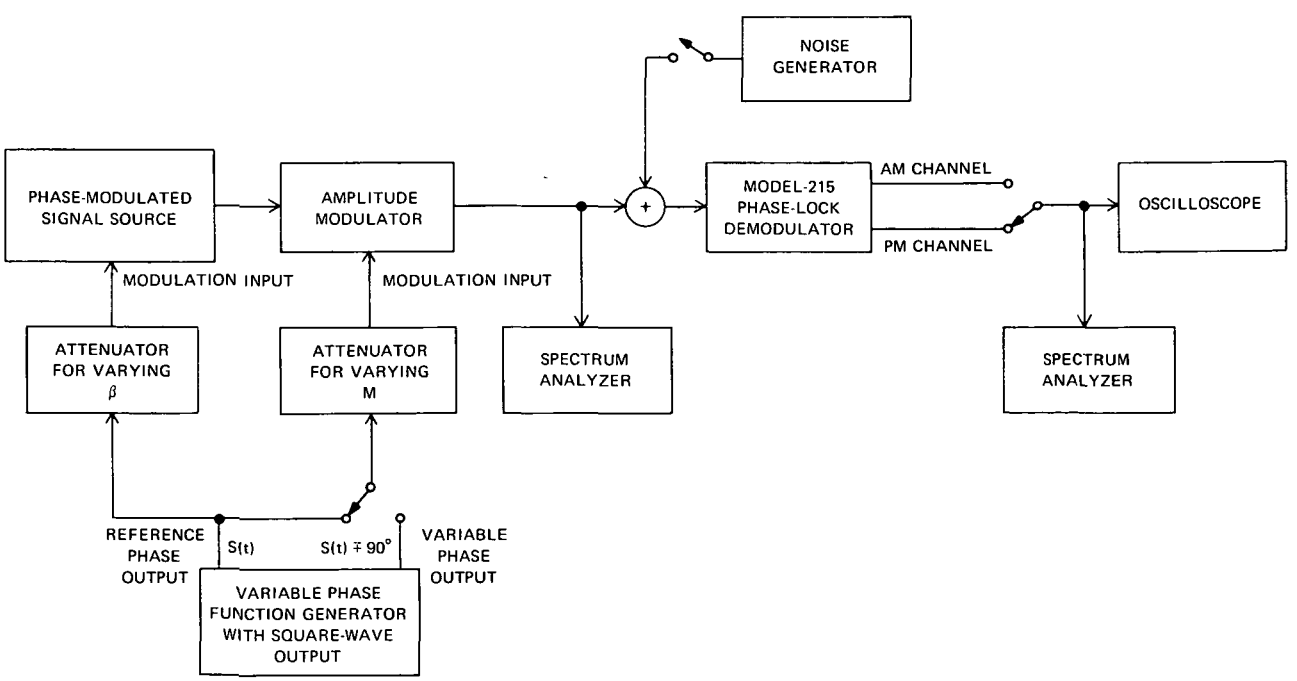

Figure 2—Test setup for study of incidental AM.

switch so that it can be driven from either the reference phase output or the variable phase output. This arrangement permits the signal applied to the AM modulator to be shifted in phase relative to the signal applied to the phase modulator.

The block diagram of the receiver, a Model-215 Electrac phase-lock demodulator, is shown in Figure 3. The demodulator is a superheterodyne phase-lock receiver employing a third-order carrier tracking loop. The third-order loop makes the receiver ideal for tracking satellites whose trajectories cause large changes in the velocity relative to the receiving station. The automatic gain control (AGC) system is coherent; i.e., it responds only to the signal carrier level. Both the AGC system and the carrier tracking loop have adjustable bandwidths to provide variable dynamic responses. Separate detectors are utilized for demodulation to provide two signal outputs. The first output, the AM channel in Figure 3, consists of the modulation components of the signal which are in phase with the signal carrier; the second output, derived from a phase detector, provides a phase demodulation channel consisting of modulation components which are in quadrature with the signal carrier.

When taking measurements of the receiver outputs with the test set-up, the carrier input to the receiver will be maintained at a fixed frequency and be well above the noise level at the receiver input. Under these conditions, the carrier tracking-loop error voltage (Figure 3) and corresponding error phase angle will be zero. This angle will be taken as zero when analyzing the demodulation process in Appendix A. The carrier tracking-loop bandwidth will be maintained at a setting of 30 Hz for all measurements; this setting is typical for most station operating conditions. The carrier tracking bandwidth, controlled by adjusting the networks in the passive and active integrators, determines the dynamic response of the receiver to changing carrier frequency as well as the ability to maintain lock in the presence of noise. The tracking bandwidth also sets a lower limit on the PM frequency at the transmitter. For a bandwidth of 30 Hz, the minimum modulation frequency is approximately 100 Hz according to the curve plotted in Figure 4, which shows the receiver PM channel output versus the modulating frequency of the phase-modulated signal source (Figure 2). Below 100 Hz, the decrease in output indicates that modulation components of the signal are entering the carrier tracking loop and modulating the receiver voltage-controlled oscillator (VCO).

The signal carrier level at the receiver input will also affect the demodulation process. In the test procedure, the carrier input level will be maintained at a level lying within the flat portion of the AGC characteristic shown in Figure 5. The flat portion of the curve corresponds to the effective control range. Within this range, the carrier amplitude at the loop phase detector remains constant; as a consequence, the carrier tracking-loop bandwidth is independent of the input signal level. Within the control range, the AGC of this receiver is very effective; the actual variation of the carrier level over the entire range is not more than a few percent. In the analysis of the demodulation process (Appendix A), the controlled carrier level will be assumed to be constant or, in equivalent terms, the AGC error voltage will be assumed to be zero.

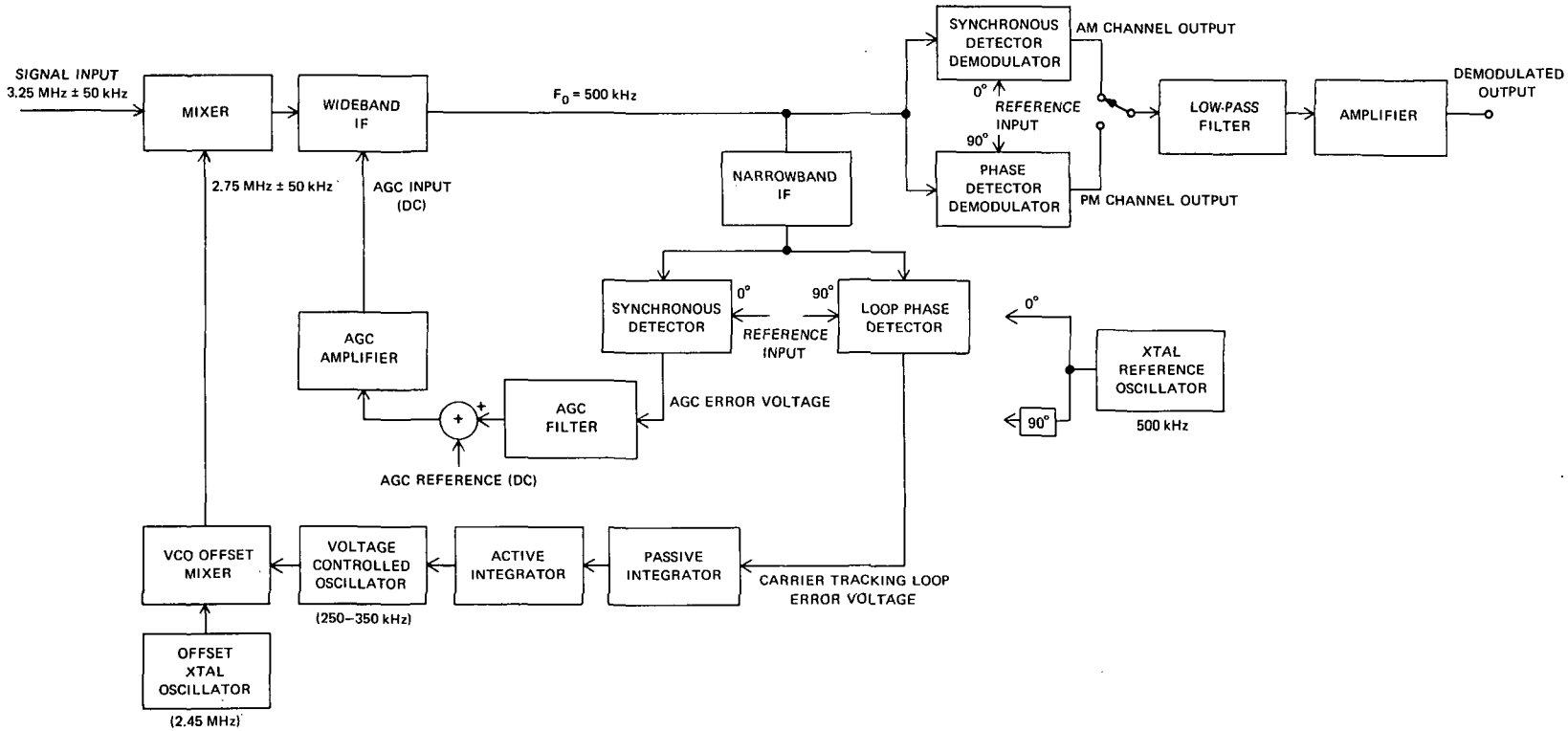

Figure 3—Block diagram of Model-215 phase-lock demodulator.

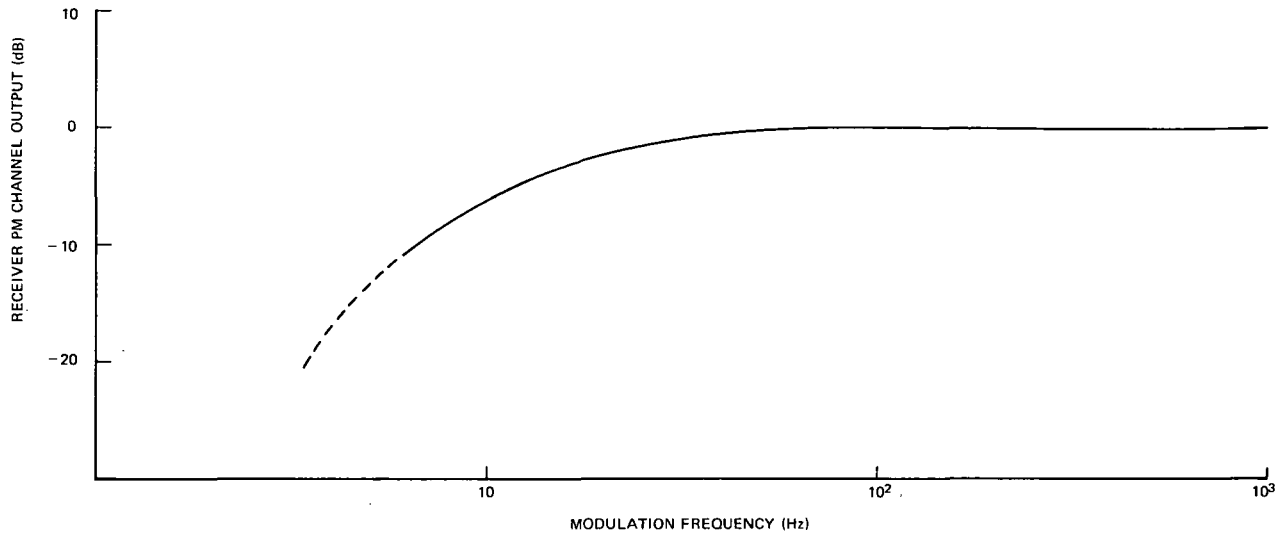

Figure 4—Low-frequency demodulation characteristic at receiver operating-loop bandwidth (30 Hz).

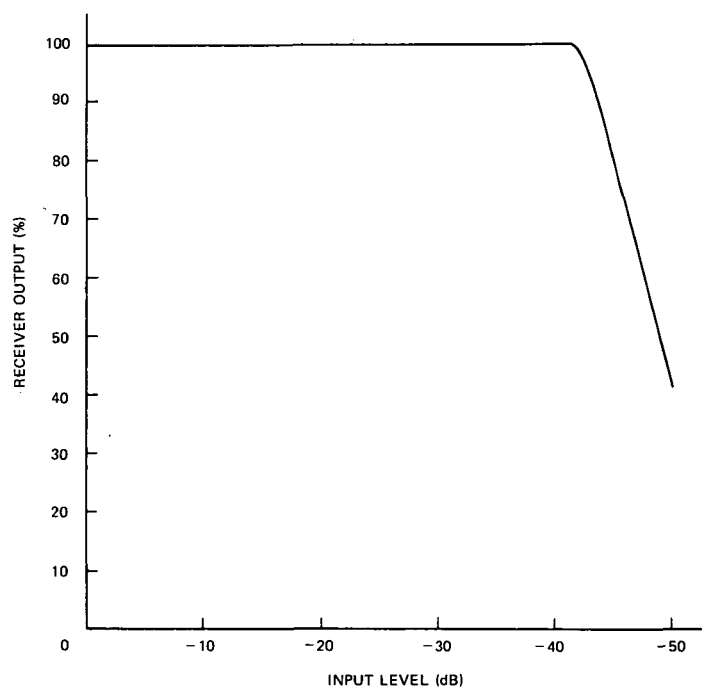

Figure 5—Receiver AGC characteristics.

CHAPTER 3

CASE I: QUADRATURE AM

Case I will be concerned with quadrature square-wave incidental AM with the signal form $E[1 + ML(t + P/4)] \cos[\omega_c t + \beta L(t)]$, where the periodic modulating signals are defined within the period P as follows:

$$\text{Quadrature AM signal } L(t+P/4) = \begin{cases} +1, & \text{for } 0 < t < \frac{P}{4} \\ -1, & \text{for } \frac{P}{4} < t < \frac{3P}{4} \\ +1, & \text{for } \frac{3P}{4} < t < P \\ \cdots \end{cases}$$

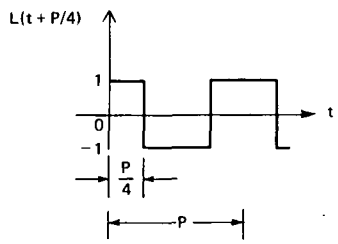

$$\text{PM modulating signal } L(t) = \begin{cases} +1, & \text{for } 0 < t < \frac{P}{2} \\ -1, & \text{for } \frac{P}{2} < t < P \\ \cdots \end{cases}$$

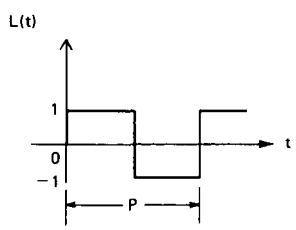

When this signal was demodulated with the type of receiver shown in Figure 3, the principal effect of the presence of incidental AM was to generate a double-frequency distortion term in the PM channel output; the PM content of the signal $\beta L(t)$ was not suppressed. The presence of incidental AM in the signal is readily detectable from the signal spectrum since the AM causes asymmetry.

Test data for this case are shown in Figure 6. The normal PM spectrum without incidental AM is given in Part A for a PM index β of 0.785 radians (45 degrees). The normal spectrum is symmetrical about the carrier ω_c with odd-order sidebands spaced at $\pm\omega_a, \pm 3\omega_a, \ldots$, relative to the carrier Part C of Figure 6 shows the spectrum of the same signal when quadrature incidental AM is present.

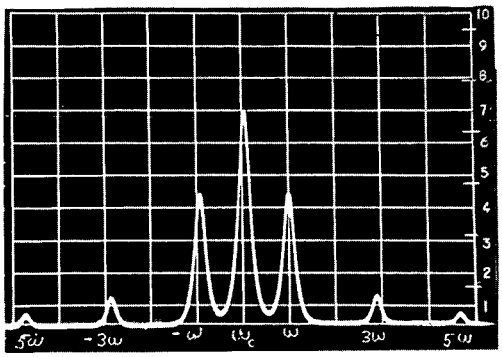

(A) Spectrum for normal PM only ($\beta = 45°$).

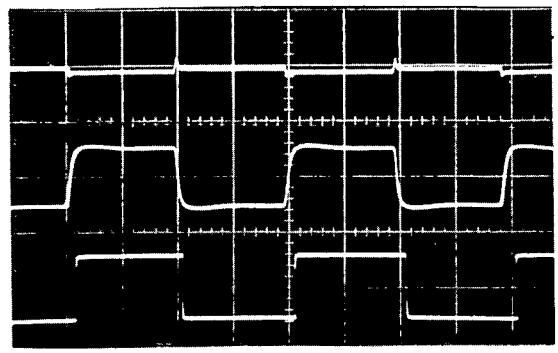

(B) Receiver outputs for normal PM only ($\beta = 45°$).

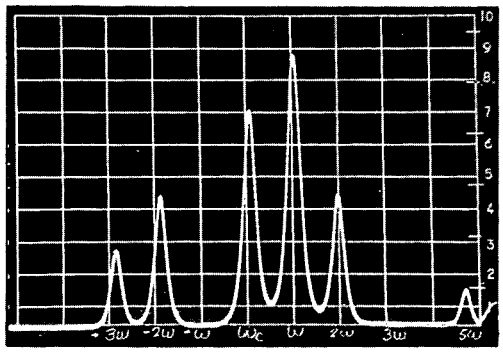

(C) Spectrum for 100-percent AM in quadrature ($\beta = 45°$).

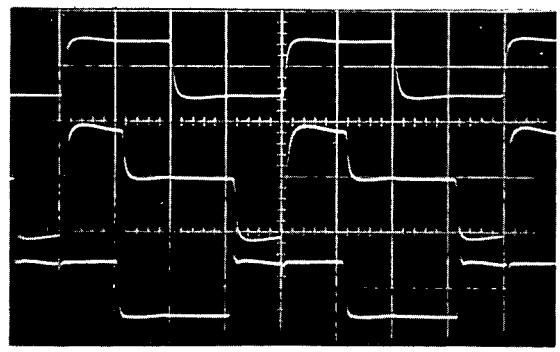

(D) Receiver outputs with 100-percent AM in quadrature (two lower traces).

Figure 6—Receiver outputs and input signal spectra.

The spectrum becomes asymmetrical; for this particular value of β, with 100 percent AM ($M = 1$), the lower sideband at $-\omega_a$ is cancelled, and the upper sideband at $+\omega_a$ is doubled in amplitude. An additional effect of the AM is to generate even-order sidebands at $\pm 2\omega_a, \pm 6\omega_a, \ldots$. The corresponding receiver outputs are shown in Part D. The receiver outputs resulting from the normal PM signal (Part A) are given by the upper traces of Part B, while the lower trace shows the input to the phase modulator (Figure 2). The PM channel output is identical to the original modulating signal except for somewhat rounded edges, while the AM channel output shows a small transient coinciding with carrier phase transition. The small transient results because the time between carrier phase transition from $+\beta$ to $-\beta$ is not actually zero, a result of bandwidth limitations in the phase modulator. The receiver output that results when 100 percent incidental AM is present is shown by the center and lower traces of Part D. The center trace is the waveform which results when the double-frequency distortion term is added to the square wave normally present from the PM content of the signal. The lower trace, the AM channel output, is the wave form $L(t + P/4)$. The effects shown are proportional to the degree of AM present, being maximum in this instance since the AM modulation index M is 1. These effects will

be treated quantatively in the following development, which will give the theoretical expression for the receiver outputs as well as the signal spectrum.

The theoretical spectrum for this case is given in Part B of Figure 7, while Part A of the same figure is the spectrum for normal PM. (The derivation is given in Appendix C.) A comparison of the two plots indicates that the presence of incidental AM alters the normal spectrum by the superposition of a term $\pm M \cos\beta$ on all odd-order spectral lines. Because the sign of this term alternates with respect to the upper and lower sidebands, the spectrum becomes asymmetrical; in the case of the measured spectrum (Part C of Figure 6) for which $M = 1$ and $\beta = 45°$, the lower sideband at $-\omega$ is completely cancelled since its amplitude, given by $\sin\beta - M\cos\beta$, is zero. In addition to the alteration in symmetry, components not normally present appear at $\pm 2\omega_a$, $\pm 6\omega_a$, . . . , with an amplitude proportional to $M \sin\beta$. The carrier amplitude, however, remains unchanged.

The signal, when written in the form of a spectrum, is useful for studies made with a spectrum analyzer, but an alternative form is more suitable when considering the demodulation process performed by the receiver. In this latter form, the signal is expressed as the sum of in-phase and quadrature components relative to the carrier; in this form, the signal can be described compactly with a phasor diagram. For example, pure square-wave PM can be written as $E \cos[\omega_c t + \beta L(t)]$, which can be partitioned into the sum $E[\cos\beta \cos\omega_c t - (\sin\beta)L(t) \sin\omega_c t]$ as in Appendix B. The phasor representation of this signal is given in Part A of Figure 8. In this diagram, the carrier $\cos\omega_c t$ is chosen as the reference phasor. The second term of the sum, the quadrature phasor containing the modulation content, is oriented upwards since $\cos(\omega_c t + 90) \equiv -\sin\omega_c t$ and the phasor rotation is taken as counter clockwise. The quadrature phasor amplitude contains the cyclic square-wave term $L(t)$ which varies

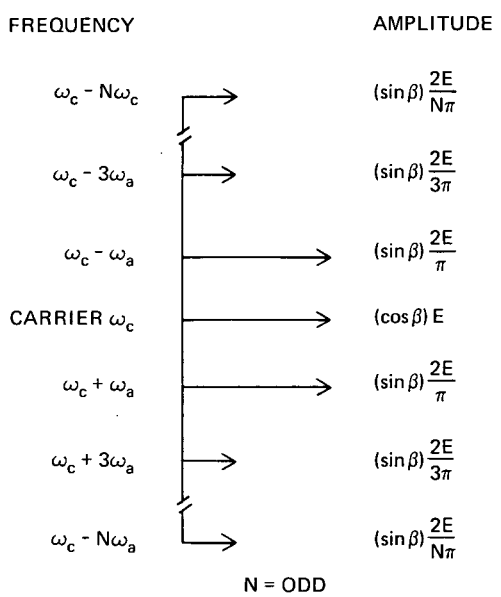

(A) Normal PM spectrum.

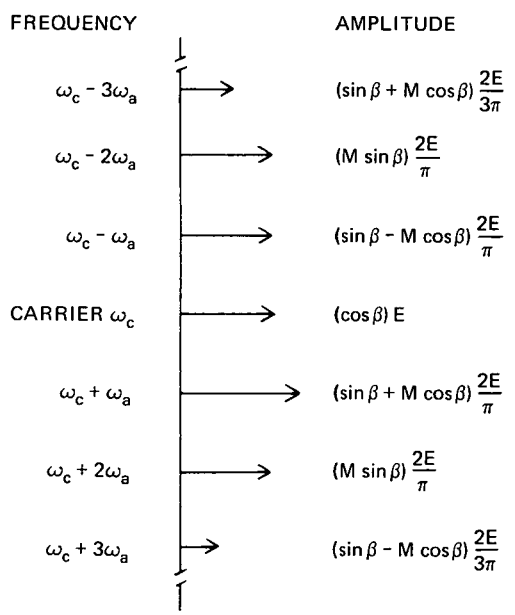

(B) PM spectrum with quadrature AM.

Figure 7—Signal spectra.

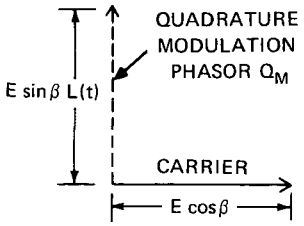

(A) Phasor diagram of input signal to receiver.

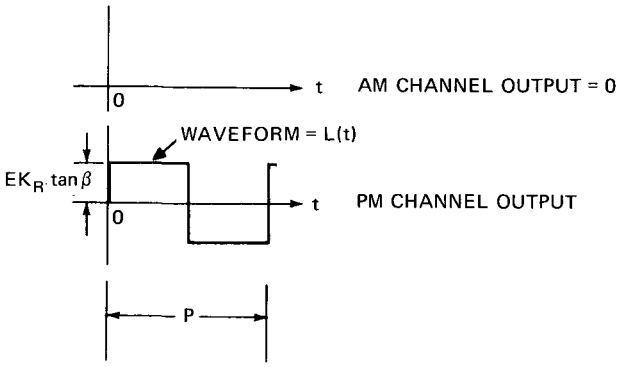

(B) Receiver AM and PM channel outputs. K_R is the receiver AGC reference (in volts).

Figure 8—Input signal phasor and corresponding receiver output for normal PM signal with square-wave modulation.

with time; consequently, it is necessary to specify time when drawing the diagram. As shown in Part A, the time interval lies in the first half of the period of $L(t)$; in the second half of the period, the quadrature phasor would point downward with the same amplitude because $L(t)$ changes sign. The theoretical receiver output, when this signal is demodulated by the receiver, is shown by Part B of Figure 8. A comparison with the phasor representation of the input signal, Part A, shows that the quadrature modulation wave form $L(t)$ appears in the PM channel, while the AM channel output is zero, there being no in-phase modulation phasor. However, the PM channel content $L(t)$ is not demodulated linearly with respect to β. In the original signal, $E\cos[\omega_c t + \beta L(t)]$, the phase deviation is directly proportional to β; the demodulated output, however, is proportional to $\tan\beta$.

Part A of Figure 9 shows the phasor diagram of a PM signal with superimposed quadrature AM. Comparison with Figure 8 shows that quadrature AM generates an additional modulation component $E(\sin\beta)ML(2t)$ in quadrature with the carrier and generates the component $E(\cos\beta)ML(t+P/4)$ in phase with the carrier. The diagram is based on Equation C.7 of Appendix C. Part B of Figure 9 shows the AM and PM channel outputs of the receiver when this signal was demodulated. As will be shown, the receiver outputs in terms of the input signal phasor are

$$\text{AM channel output} = \frac{K_R}{\text{carrier amplitude}} \Sigma(\text{in-phase modulation phasors})$$

$$\text{PM channel output} = \frac{K_R}{\text{carrier amplitude}} \Sigma(\text{quadrature modulation phasors}).$$

From the phasor diagram, Part A of Figure 9, and the above relationships, the receiver outputs are:

$$\text{AM channel output} = \frac{K_R}{E\cos\beta} EM(\cos\beta)L(t+P/4)$$

$$= K_R ML(t+P/4).$$

$$\text{PM channel output} = \frac{K_R}{E\cos\beta} E(\sin\beta)[L(t) + ML(2t)]$$

$$= K_R(\tan\beta)[L(t) + ML(2t)]\,,$$

where K_R is the receiver AGC reference voltage. The PM channel wave form is the sum of the wave form $L(t)$ having an amplitude $K_R \tan\beta$, which is the component normally present with pure PM, and the distortion component $L(2t)$ having an amplitude $MK_R \tan\beta$. The resultant sum is shown as the lower wave form in Part B. In scaling the drawing, M was taken as unity (100-percent AM); hence, the resultant is zero from $P/4$ to $3P/4$. The waveform is seen to agree with the photograph of the PM channel output of the receiver, Part D of Figure 6, made for 100-percent quadrature AM.

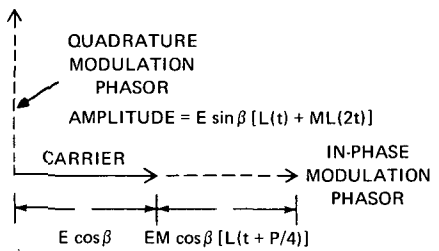

(A) Phasor diagram of input signal to receiver.

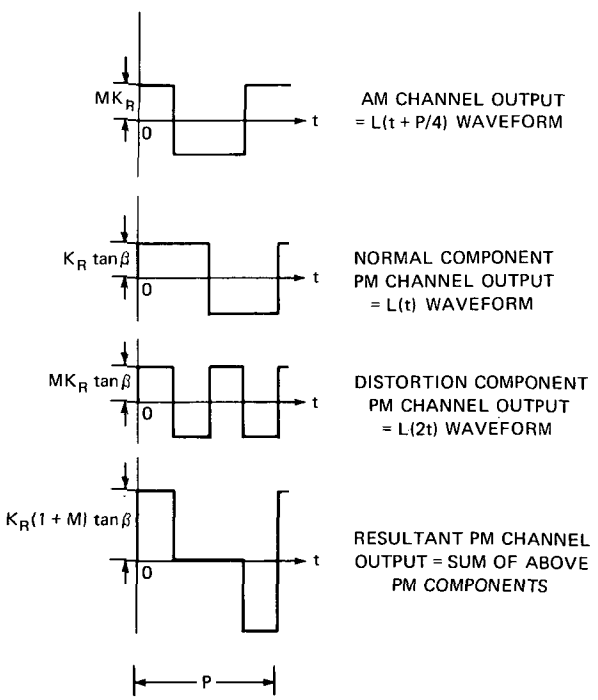

(B) Receiver AM and PM channel outputs. K_R is the receiver AGC reference (in volts).

Figure 9—Input signal phasor and corresponding receiver outputs for quadrature incidental AM.

The AM channel output $L(t + P/4)$, i.e., $L(t)$ shifted a quarter period, is directly comparable to the lower trace of the same photograph.

Calculation of the receiver outputs is based on the equivalent circuit shown in Figure 10. This circuit, derived in Appendix A, is a mathematical model of the actual receiver (Figure 3). The salient characteristics of the model are that (1) the phase and synchronous detectors, and the input mixer of the actual receiver are represented by mathematical multipliers, and (2) the equivalent circuit uses only two detectors, which combine the AM channel demodulation and the AGC function in a single detector and the PM channel demodulation and loop control in a single detector; the actual receiver uses an additional pair of detectors for the demodulation process.

To determine the demodulated outputs with the quivalent circuit, we partition the receiver input signal into in-phase and quadrature terms of the form

$$I\cos\omega_c t - Q\sin\omega_c t\,, \qquad (1)$$

where I is the in-phase factor and Q is the quadrature factor. The factor I will contain constants as well as modulation terms.

With the input signal partitioned as above, the receiver outputs as derived in Appendix A are

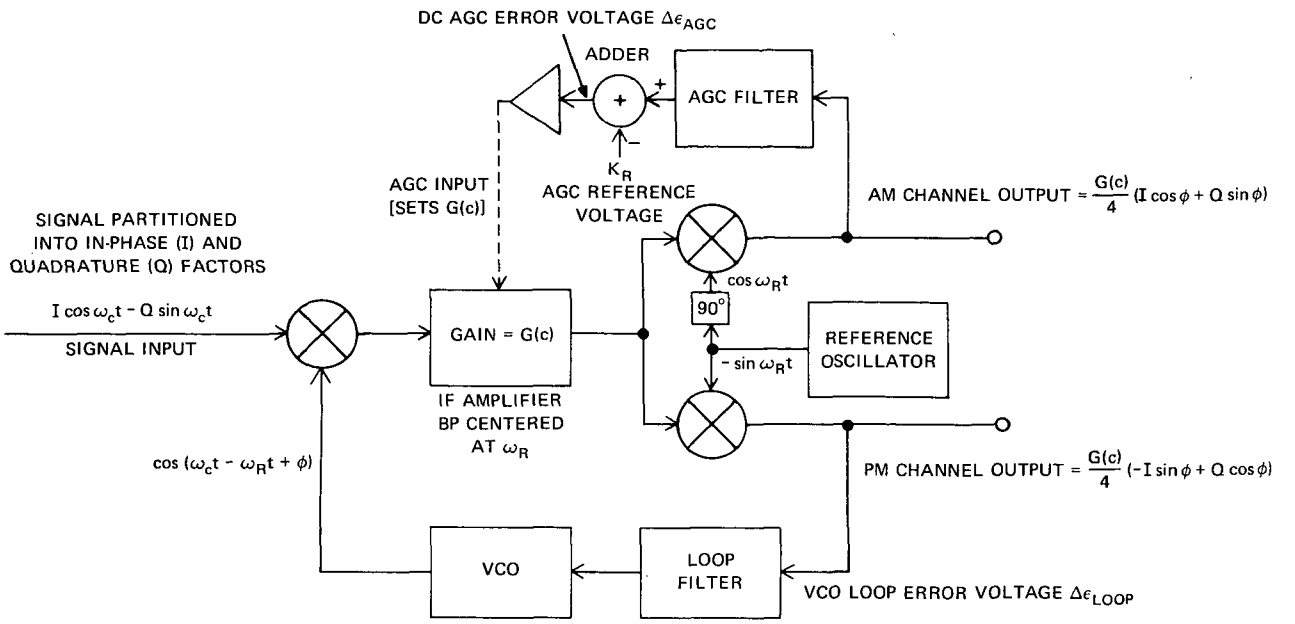

Figure 10—Equivalent circuit of receiver used for calculating AM and PM channel outputs. As shown, the system is in frequency synchronism and is not in phase lock.

$$\text{PM channel output} = \frac{G(c)}{4}(-I \sin\phi + Q \cos\phi) \tag{2}$$

$$\text{AM channel output} = \frac{G(c)}{4}(I \cos\phi + Q \sin\phi)\,, \tag{3}$$

where $G(c)$ is the receiver IF gain and ϕ is the VCO phase angle at the input to the multiplier preceding the IF amplifier (Figure 10). Given the assumption that the receiver has locked on the signal, the dependent variables ϕ and $G(c)$ are evaluated as follows: To determine ϕ, we note that the dc content present at the PM channel is the phase-lock loop error voltage $\Delta\epsilon_{loop}$, which is assumed to be zero when the receiver is in lock; i.e.,

$$\begin{aligned}\text{dc content of Equation 2} &= \Delta\epsilon_{loop} \\ &= 0 \text{ (steady state)}\,.\end{aligned} \tag{4}$$

To determine the system gain $G(c)$, we note that the dc content of the AM channel output is applied to the AGC adder where it is compared to the reference voltage K_R. The resulting difference is the AGC error voltage. Given the assumption that the AGC error voltage $\Delta\epsilon_{AGC} = 0$, the equation of the adder, from which $G(c)$ can be evaluated, is

$$\begin{aligned}(\text{dc content of AM channel}) - K_R &= \Delta\epsilon_{AGC} \\ &= 0\,.\end{aligned} \tag{5}$$

To calculate the receiver outputs for the case at hand, first, we partition the signal into in-phase and quadrature factors:

According to Equation C.7, Appendix C,

$$E[1+ML(t+P/4)]\ \cos[\omega_c t+\beta L(t)] = E\cos\beta\cos\omega_c t + E(\cos\beta)ML(t+P/4) - E[L(t)+ML(2t)]\sin\beta\sin\omega_c t\,. \tag{6}$$

This relationship is shown in phasor form by Part A of Figure 9.

According to the definitions given by Equation 1, the I and Q terms in Equation 6 are

$$\begin{aligned} I &= E(\cos\beta)ML(t+P/4) + E\cos\beta \\ Q &= E(\sin\beta)[L(t)+ML(2t)]\,. \end{aligned} \tag{7}$$

To determine the PM channel output, substitute I and Q into Equation 2:

$$\text{PM channel output} = \frac{EG(c)}{4}\left\{[L(t)+ML(2t)]\sin\beta\cos\phi - [\cos\beta+(\cos\beta)ML(t+P/4)]\sin\phi\right\}. \tag{8}$$

To determine ϕ, we note that the dc content of the PM channel output, above, is the term $-[EG(c)/4]\cos\beta\sin\phi$. This term is the VCO loop error, which is assumed to be zero as in Equation 4:

$$\begin{aligned} -\frac{G(c)E}{4}\cos\beta\sin\phi &= \Delta\epsilon_{\text{VCO loop}} \\ &= 0\,. \end{aligned}$$

Consequently, $\sin\phi = 0$, and $\phi = N\pi$, where $N = 0, 1, 2, 3, \ldots$; however, only even values of N permit stable lock. Hence,

$$\phi = 0, 2\pi, \ldots. \tag{9}$$

For ϕ to be zero requires that the modulation terms, such as $L(t)$, which appear at the PM channel be blocked by the VCO loop filter (Figure 10). In the case of the Model-215 Electrac receiver, the data plotted in Figure 4 indicate that with a VCO loop bandwidth of 30 Hz, $L(t)$ should have a fundamental frequency greater than 100 Hz.

With $\phi = 0$, the PM channel output, Equation 8, reduces to

$$\frac{G(c)}{4}Q = \frac{EG(c)}{4}[L(t)+ML(2t)]\sin\beta\,. \tag{10}$$

The AM channel output, Equation 3, reduces to

$$\frac{G(c)}{4} I = \frac{EG(c)}{4} [\cos\beta + (\cos\beta) ML(t + P/4)], \tag{11}$$

using the value for I given by Equation 7.

The dc term in the AM output which is applied AGC adder (Figure 10) is $EG(c)$ $(\cos\beta)/4$; substituting this term in Equation 4 gives

$$\frac{EG(c)\cos\beta}{4} - K_R = \Delta\epsilon_{AGC}$$

$$= 0 .$$

Solving for $G(c)$ results in:

$$G(c) = \frac{4K_R}{E\cos\beta}, \tag{12}$$

which is to say that the system gain $G(c)$ is inversely proportional to the input signal carrier amplitude $E\cos\beta$. This relationship depends upon the assumption that the AGC error is zero. In the actual receiver, the AGC error cannot be zero since this would imply infinite gain in the AGC amplifier. However, the measured AGC characteristic, Figure 5, shows that the AGC gain is exceedingly large (the loop gain is inversely proportional to the slope of the straight-line portion of the plot). In Equation 11, it is assumed that the cyclic modulation term $L(t + P/4)$ is precluded by the AGC filter (Figure 10) from appearing at the AGC adder.

Finally, to obtain the desired receiver AM and PM outputs, we substitute the equivalent for $G(c)$ in Equation 12 into Equations 10 and 11. This gives the outputs in terms of the input signal I and Q factors:

$$\begin{matrix}\text{AM channel output} \\ \text{including dc terms}\end{matrix} = \frac{K_R}{\text{carrier amplitude}} I$$

$$= K_R + K_R ML(t + P/4) \tag{13}$$

$$\text{PM channel output} = \frac{K_R}{\text{carrier amplitude}} Q$$

$$= K_R \tan\beta [L(t) + ML(2t)] . \tag{14}$$

The AM channel output contains the dc term K_R because the inphase factor I includes the carrier as well as modulation components of the signal. If only the ac components of the demodulated signal are desired, we replace I in Equation 13 with I_M, where I_M represents the modulation components in phase with the carrier. Equations 13 and 14 form the basis for the receiver outputs shown in Part B of Figure 9.

CHAPTER 4

CASE II: IN-PHASE INCIDENTAL AM

Case II will be concerned with a signal, simultaneously phase and amplitude modulated, from a single square-wave source. For this case, the signal expression can be written

$$E[1 + ML(t)] \cos [\omega_c t + \beta L(t)] ,$$

where β and M represent the PM and AM indexes. As has been noted previously, a signal of this type is most probable if incidental AM occurs in phase-modulated transmitters. The most significant effect that results from this type of AM is the suppression of the PM content of the signal. This type of incidental AM is not easily detected from the signal spectrum because the spectral symmetry characteristic of the normal PM signal is not changed by the presence of incidental AM.

The suppression effect and spectrum of this signal are demonstrated by the photographs in Figure 11. These data were obtained with the test set-up (Figure 2). The receiver input signal spectrum and receiver outputs for a normal square-wave phase-modulated signal with $\beta \approx 1$ rad are shown in Parts A and B. The effect of the superposition of 100-percent AM on the same signal is shown in Parts C and D. The receiver PM channel output is seen to be completely suppressed, while the receiver AM channel output (zero for normal square-wave PM) shows a square-wave output. The signal modulation has, in fact, been converted to pure AM. With the superposition of 100-percent AM, the spectrum remains symmetrical and shows an increase in amplitude of the carrier and all sidebands; no new sideband frequencies result.

Signal Spectrum

Part B of Figure 12 shows the theoretical spectrum for in-phase incidental AM; the derivation is given in Appendix D. For comparison, the spectrum for normal square-wave PM is shown in Part A. As is evident from the figure, in-phase incidental AM causes the quadrature addition of the term $M^2 \sin^2 \beta$ to the normal carrier amplitude and the addition in quadrature of $M^2 \cos^2 \beta$ to the normal sideband terms. The normal spectrum is otherwise unchanged. Because these AM generated terms are added in quadrature, and are proportional to M^2, the change in spectral amplitudes for small values of the AM index M is very slight. Consequently, spectral analysis is not the best method for detecting in-phase incidental AM. Alternative methods, such as viewing the envelope of the signal with an oscilloscope, are preferable.

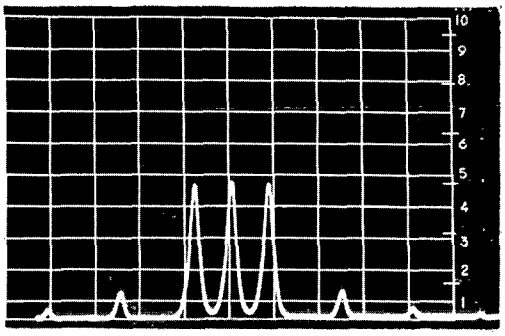

(A) Receiver input signal spectrum for no AM ($\beta \approx 1$ rad).

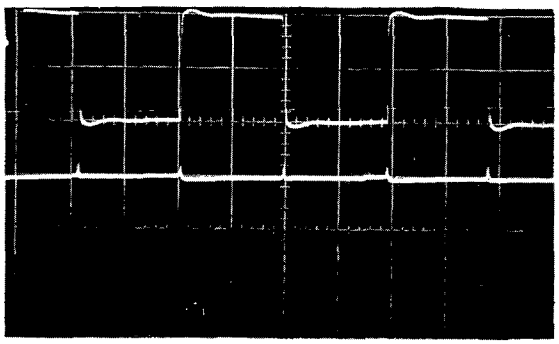

(B) Receiver PM and AM channel outputs corresponding to signal in Part A.

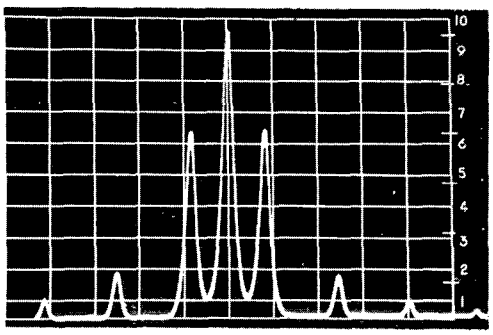

(C) Receiver input signal spectrum with 100-percent incidental AM ($\beta = 1$ rad).

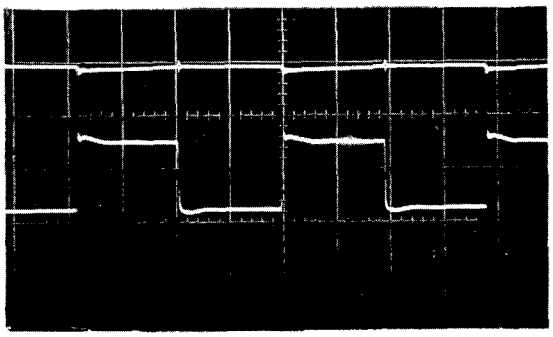

(D) Receiver PM and AM channel outputs corresponding to signal in Part C.

Figure 11—Receiver input signal spectra and corresponding outputs showing the effect of 100-percent incidental in-phase AM.

Signal Phasor Diagram

The suppressive effect of superimposed in-phase incidental AM on the PM channel output of the receiver shown in the photographs of Figure 11 results primarily because this type of AM generates a carrier component which is in quadrature with the normal carrier. The quadrature carrier component causes an increase in the resultant carrier amplitude, but more importantly, causes a phase shift of the carrier with respect to the modulation components of the signal. It is the phase orientation of the carrier with respect to the modulation content of the signal which determines the receiver output: Modulation components in phase with the carrier appear at the AM channel output; modulation components in quadrature with the carrier appear at the PM channel output. In the case of the data shown in previous photographs when the AM index was 100 percent ($M = 1$), the carrier alignment is such that the quadrature components cancelled, with the result that the PM channel of the receiver showed no output. To predict this process for any value of M, it is necessary to compute the signal quadrature and in-phase modulation components with respect to the resultant carrier. Analytically, this can be

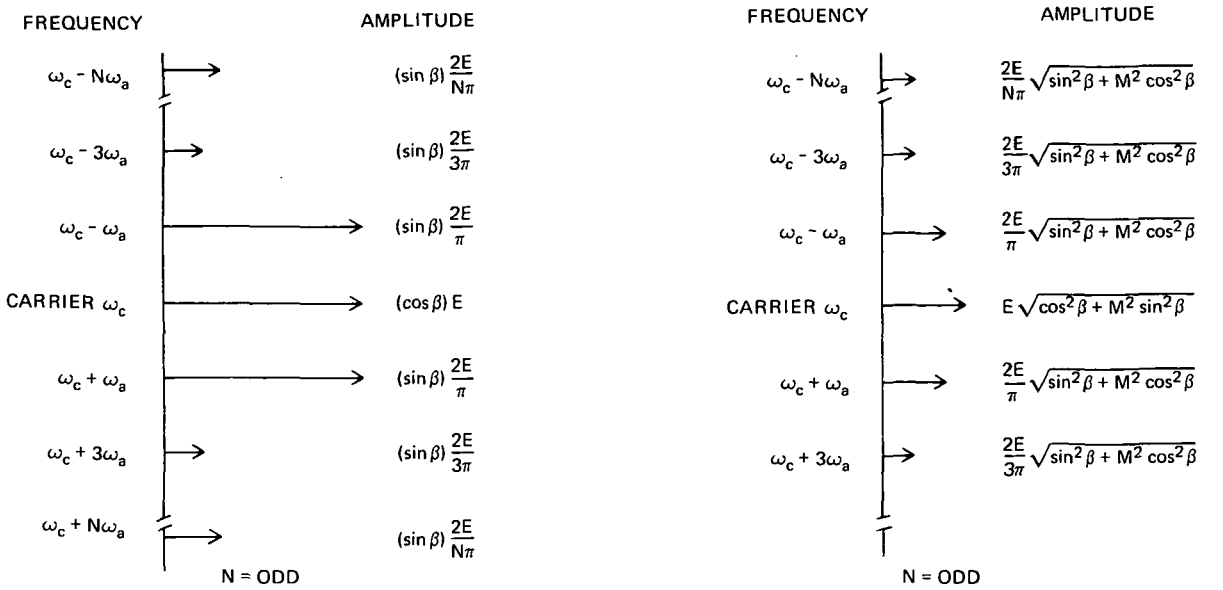

(A) Normal PM spectrum.

(B) Spectrum of PM signal with in-phase AM.

Figure 12—Signal spectra with square-wave modulation.

done most simply from the phasor representation of the signal; once the phasor representation of the signal with the resultant carrier as the reference is determined, the receiver output can be predicted immediately. The signal expression

$$E[1 + ML(t)]\cos[\omega_c t + \beta L(t)]$$

is expanded as follows (see Equation D.4, Appendix D):

$$E_{\text{signal}} = E\cos\beta\cos\omega_c t - EM\sin\beta\sin\omega_c t + I_M\cos\omega_c t - Q_M\sin\omega_c t\,, \tag{15}$$

where

$$I_M = EL(t)M\cos\beta$$

$$Q_M = EL(t)\sin\beta.$$

The terms Q_M and I_M represent the quadrature and in-phase modulation content of the signal with respect to the carrier component $\cos\omega_c t$. Initially, we choose $\cos\omega_c t$ as the reference phasor aligned with the real axis. The phasors representing $-\sin\omega_c t$ (Equation 15) will lie on the $+j$ axis since

$$\cos\left(\omega_c t + \frac{\pi}{2}\right) \equiv -\sin\omega_c t$$

and operationally $+j$ is equivalent to a phasor rotation of $+\pi/2$ rad. The phasor diagram with $\cos\omega_c t$ as the reference phasor is shown by Part A of Figure 13. In this diagram, the phasors representing the carrier (the first two terms of Equation 15) are drawn with solid lines, while phasors representing the terms Q_M and I_M (Equation 15) are drawn as dotted lines. These phasors have an amplitude proportional

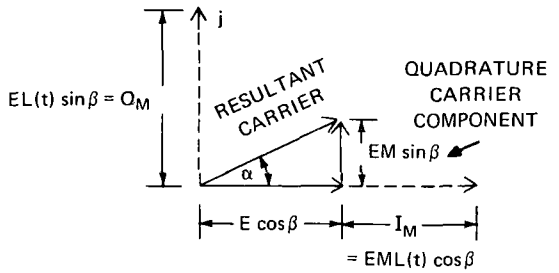

(A) Signal phasor with carrier component cos $\omega_c t$ as reference phasor.

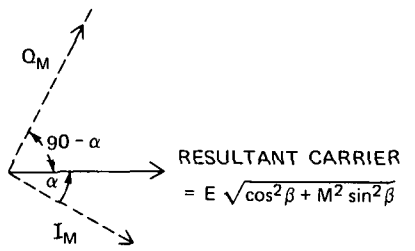

(B) Signal phasor system rotated so as to make resultant carrier the reference phasor.

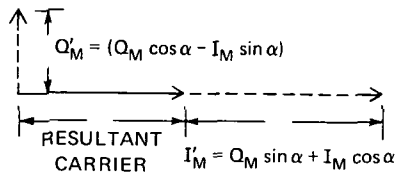

(C) New modulation phasors Q'_m and I'_m orthogonal to resultant carrier. Q'_m and I'_m were obtained from Part B by projection.

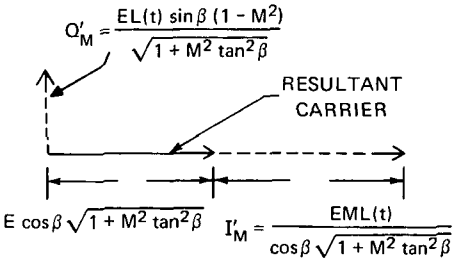

(D) Final signal phasor system after eliminating α from Part C. Note, from Part A, that tan $\alpha = M$ tan β.

Figure 13—Development of phasor diagram for in-phase square-wave incidental AM.

to the square-wave modulation term $L(t)$ and will periodically reverse direction; as drawn, the direction corresponds to periods of time when $L(t)$ is positive. The resultant carrier shown in the diagram is the vector sum of the quadrature component $EM \sin\beta$ generated by incidental AM, and the carrier component $E \cos\beta$ which was selected as the reference. To determine the in-phase and quadrature components of the modulation with respect to the resultant carrier, we rotate the phasors system α deg to make the resultant carrier the reference phasor. The phasor system will then appear as in Part B of Figure 13, where Q_M makes an angle $90 - \alpha$ deg with respect to the resultant carrier and I_M makes an angle of $-\alpha$ deg. We define I'_M as the in-phase modulation component and Q'_M as the quadrature modulation component with respect to the resultant carrier. Q'_M and I'_M are then determined by projecting Q_M and I_M on the j and real axes of Part B. (See Equations D.8 and D.9, Appendix D). Projection results in

$$\begin{aligned} Q'_M &= Q_M \cos\alpha - I_M \sin\alpha \\ &= EL(t) \sin\beta \cos\alpha - EL(t)M \cos\beta \sin\alpha \\ I'_M &= I_M \cos\alpha + Q_M \sin\alpha \\ &= EL(t) \sin\beta \sin\alpha + EL(t)M \cos\beta \cos\alpha . \end{aligned} \tag{16}$$

The phasor diagram with Q'_M and I'_M as defined above is shown in Part C of Figure 13. The projection functions $\cos\alpha$ and $\sin\alpha$ (Equation 16) can be evaluated from the triangle forming the resultant carrier in Part A of Figure 13. Namely,

$$\cos\alpha = \frac{\cos\beta}{\sqrt{\cos^2\beta + M^2\sin^2\beta}}$$

$$\sin\alpha = \frac{M\sin\beta}{\sqrt{\cos^2\beta + M^2\sin^2\beta}}. \tag{17}$$

We substitute the above into Equation 16 to give

$$Q'_M = \frac{EL(t)(\sin\beta)(1-M^2)}{\sqrt{1+M^2\tan^2\beta}}$$

$$I'_M = \frac{EL(t)M}{\cos\beta\sqrt{1+M^2\tan^2\beta}}. \tag{18}$$

I'_M and Q'_M are shown in Part D of Figure 13. The equation corresponding to this phasor diagram can be written as

$$E_{\text{signal}} = E(\cos\beta)\sqrt{1+M^2\tan^2\beta}\cos\omega_c t + I'_M\cos\omega_c t - Q'_M\sin\omega_c t\,. \tag{19}$$

Receiver Output With In-Phase AM

In Case I, it was shown that if the receiver input signal is first expressed in phasor form showing in-phase and quadrature modulation components, the demodulated outputs in terms of the input signal are

$$\text{AM channel demodulated output} = \frac{K_R}{\text{carrier amplitude}}\,\Sigma(\text{in-phase modulation phasors})$$

$$\text{PM channel demodulated output} = \frac{K_R}{\text{carrier amplitude}}\,\Sigma(\text{quadrature modulation phasors}) \tag{20}$$

(K_R is the AGC reference voltage). For use in the above relationships, the phasor form of the input signal with in-phase incidental AM (Equation 19) will be repeated for clarity:

$$E[1+ML(t)]\cos[\omega_c t + \beta L(t)] = E(\cos\beta)\sqrt{1+M^2\tan^2\beta}\cos\omega_c t + I'_M\cos\omega_c t - Q'_M\sin\omega_c t\,,$$

where

$$E(\cos\beta)\sqrt{1+M^2\tan^2\beta} = \text{carrier amplitude}$$

$$I'_M = \frac{EM}{\cos\beta\sqrt{1+M^2\tan^2\beta}}L(t) \qquad \text{(in-phase modulation phasor)}$$

$$Q'_M = \frac{E(\sin\beta)(1-M^2)}{\sqrt{1+M^2\tan^2\beta}}L(t) \qquad \text{(quadrature modulation phasor).}$$

Substituting the above definitions for I'_M, Q'_M, and carrier amplitude into Equation 20, the expression for receiver outputs, gives the demodulated receiver outputs for in-phase incidental AM:

$$\text{AM channel demodulated output} = \frac{K_R M}{\cos^2\beta\,(1 + M^2\tan^2\beta)}L(t) \tag{21}$$

$$\text{PM channel demodulated output} = \frac{K_R(\sin\beta)(1 - M^2)}{\cos\beta\,(1 + M^2\tan^2\beta)}L(t)\,. \tag{22}$$

The fundamental frequency of the square wave $L(t)$ in the preceding expressions is presumed to be above the receiver VCO and AGC servo-loop bandpass frequencies.

Equations 21 and 22 are illustrated in Part B of Figure 14; the input signal phasor is diagramed in Part A. From the diagram, it is evident that the wave form $L(t)$ appears in both output channels of the receiver with phase coincidence when the input signal is

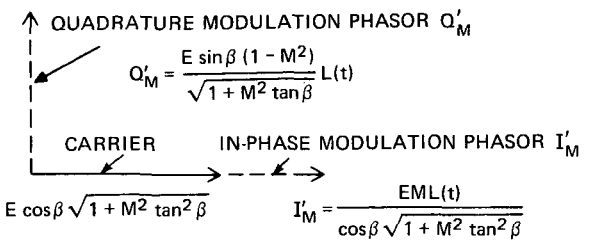

(A) Phasor diagram.

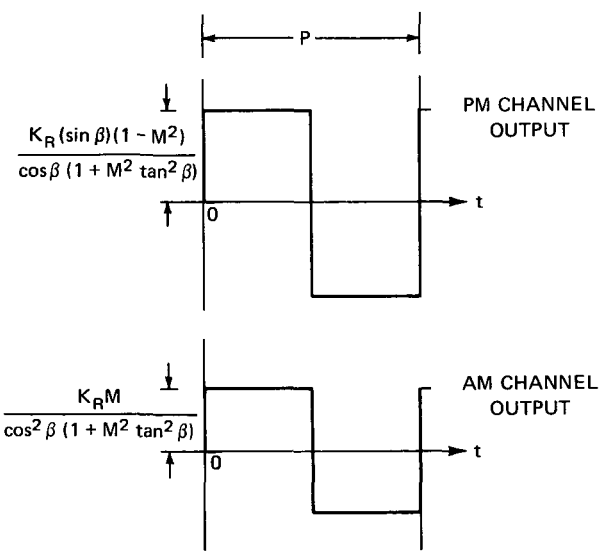

(B) Receiver outputs.

Figure 14—Input signal phasor diagram and receiver output for in-phase AM.

$$E[1 + ML(t)]\cos[\omega_c t + \beta L(t)]\,.$$

If the input signal is

$$E[1 - ML(t)]\cos[\omega_c t + \beta L(t)]\,,$$

as was the case for the transmitter (Figure 1), we replace M with $-M$ in Equations 21 and 22. The PM channel output will remain unchanged since M appears in squared form. The demodulated AM channel output and the square wave $L(t)$ will reverse phase: If the receiver input is

$$E[1 - ML(t)]\cos[\omega_c t + \beta L(t)]\,,$$

then,

$$\text{AM channel demodulated output} = -\frac{K_R M}{\cos^2\beta\,(1 + M^2\tan^2\beta)}L(t)$$

$$\text{PM channel demodulated output} = \frac{K_R(\sin\beta)(1 - M^2)}{\cos\beta\,(1 + M^2\tan^2\beta)}\,.$$

Equations 21 and 22 are plotted in Figure 15 with peak amplitude as the ordinate and M as the abscissa for three values of β: 38, 57.52, and 70 deg. The AGC factor K_R in the numerator of these equations has been taken arbitrarily to be unity for making the plots. An inspection of the

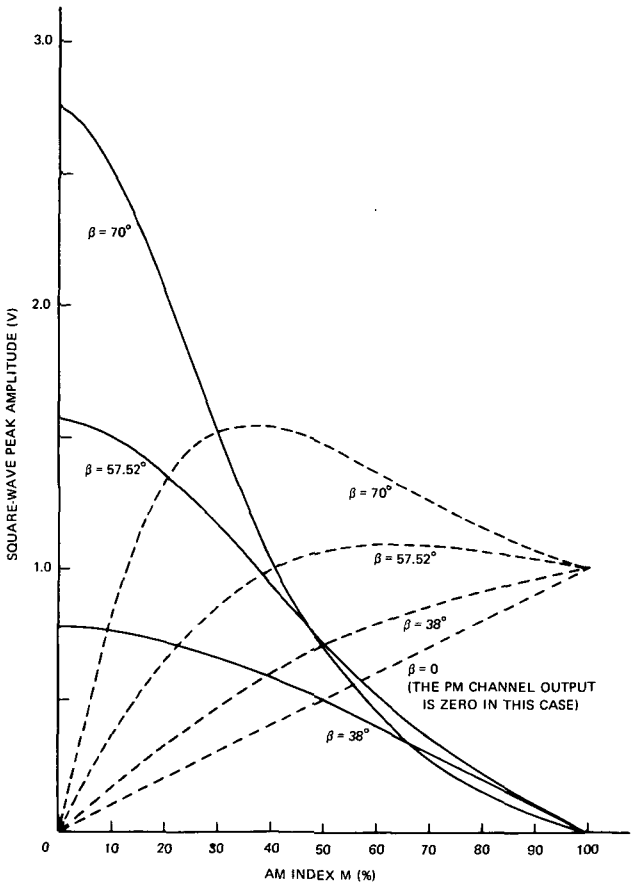

Figure 15—Theoretical receiver outputs versus AM index M for β = 0, 38, 57.52, and 72 deg. The input signal is given by $E[1 + ML(t)] \cos[\omega_c t + \beta L(t)]$, and the AGC reference $K_R \approx 1$ V. The solid and dotted curves show the square-wave outputs of the PM and AM channels, respectively.

plots shows that for the smaller value of β (38 deg), the shape of both curves is determined essentially by the numerator of the corresponding equation. Consequently the PM channel square-wave amplitude decreases as $1 - M^2$, as in Equation 22, while the AM channel square-wave amplitude increases as M, the numerator of Equation 21. For larger values of β, the term $1 + M^2 \tan^2 \beta$ in the denominator of both expressions becomes increasingly significant. Because this term increases as M increases and is proportional to $\tan^2 \beta$, the PM channel output falls much more rapidly at the higher values of β. As β approaches 90 deg, the slope becomes essentially vertical.

The slope of the AM channel output is also reduced by the effect of the denominator; at $\beta = 0$, the slope is unity. At higher values of β, the slope is increasingly reduced, as evidenced by the increase in curvature.

The AM and PM channel outputs predicted by Equations 21 and 22 are compared with measured values in the data shown by Figures 16, 17, and 18. For plotting predicted values, Equations 21 and 22 were normalized first with respect to the PM channel output for zero incidental AM ($M = 0$). The PM channel output (Equation 22) is $K_R(\tan\beta)L(t)$ for $M = 0$. With this value, the normalized receiver outputs in percent of peak amplitude of the wave form $L(t)$ are found by dividing the right hand portions of both Equations 21 (for the AM output) and 22 (for the PM output) by $K_R(\tan\beta)L(t)$ and multiplying by 100. Thus:

$$\text{Normalized AM channel output percent} = \frac{M(1 + \tan^2\beta)}{(1 + M^2 \tan^2\beta)\tan\beta} \times 100 \qquad (23)$$

$$\text{Normalized PM channel output percent} = \frac{1 - M^2}{1 + M^2 \tan^2\beta} \times 100\,. \qquad (24)$$

The above normalized equations are plotted as solid lines in each of the figures, with percent as the ordinate and the AM index M as the abscissa. Each figure corresponds respectively to β = 38, 57.52, and 70 deg. Measured values made with the test set-up (Figure 2) are shown as circles in each of the three figures. The agreement between measured and predicted values of the AM channel output is very

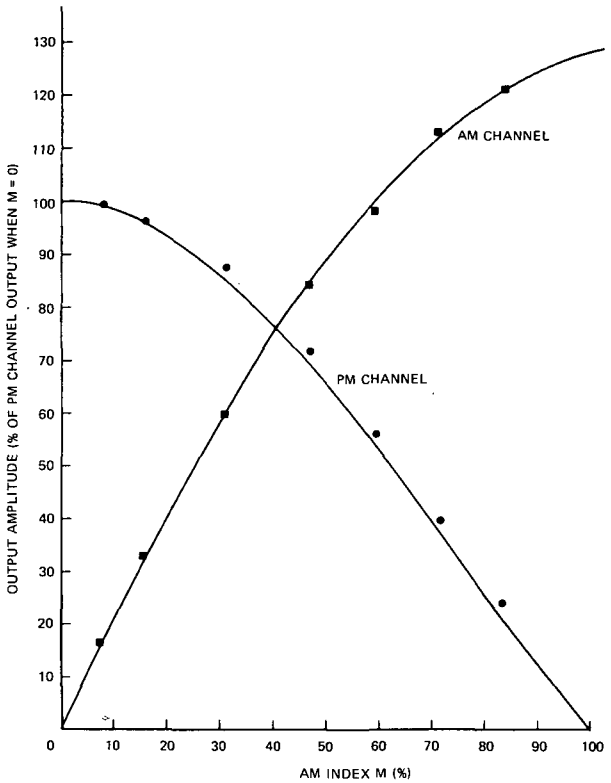

Figure 16—Normalized receiver outputs versus AM index M for β = 38 deg. The data points show measured values; the curves show theoretical predictions.

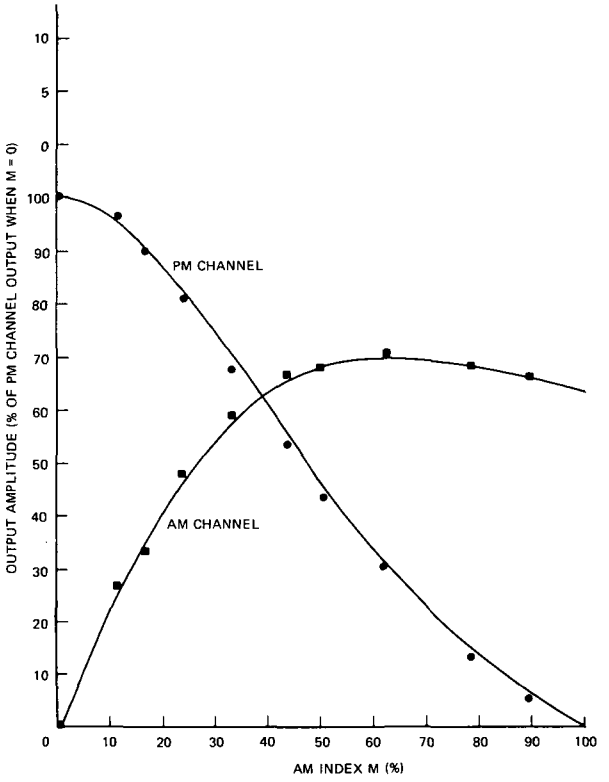

Figure 17—Normalized receiver outputs versus AM index M for β = 57.52 deg. The data points show measured values; the curves show theoretical predictions.

close in each of the figures. The agreement in the case of the PM channel output is not as close; however, the discrepancies are not large enough to be considered significant.

Effect of Incidental AM on Signal-to-Noise Power Ratio at Receiver Output

In this section, the S/N power ratio at the receiver output will be determined as a function of the AM index M when the input signal contains in-phase incidental AM;

$$E_{\text{signal}} = E[1 + ML(t)] \cos [\omega_c t + \beta L(t)] .$$

The input noise will be assumed to be white Gaussian noise with a power density of η W/Hz. The effects of noise on the AGC and VCO loops of the receiver will not be considered.

The analysis follows from the signal flow path of the receiver diagramed in Part A of Figure 19. The receiver is represented by an input multiplier where the signal is multiplied by the VCO input; the multiplier is followed by a wideband amplifier with gain $G(c)$ which feeds the IF amplifier. The IF amplifier is assumed to have a rectangular frequency aperture with unity gain. The output of the IF amplifier is applied to the AM and PM detectors, represented as multipliers, where the signal is

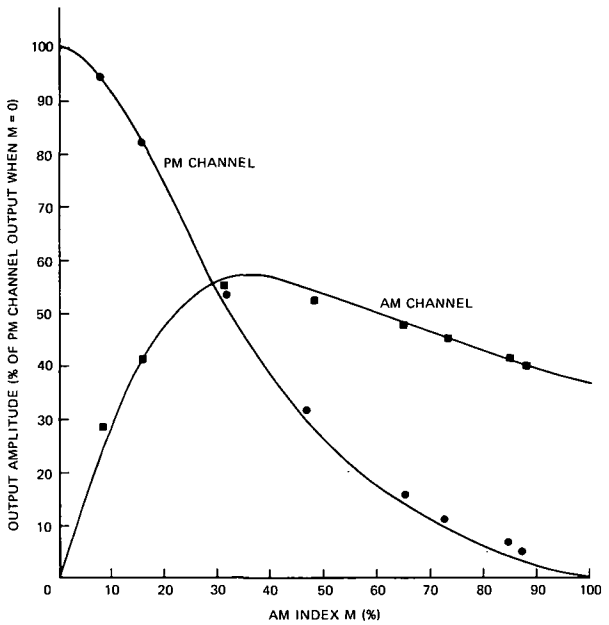

Figure 18—Normalized receiver outputs versus AM index M for β = 70 deg. The data points show measured values; the curves show theoretical predictions.

demodulated through multiplication by quadrature and in-phase inputs obtained for the reference oscillator with frequency ω_R. Since the analysis consists of determining the voltage at the junction between each unit in the signal flow path, it will be necessary to specify impedances. To simplify the analysis, each unit in the signal flow path will be assumed to be noiseless and to be operated under matched conditions; namely, the output resistance R_s shall be equal to the input resistance R_l of the succeeding unit. Further, R_s will be assumed to be identical for each unit and have a value of 0.25 Ω. The voltage at each junction, e_K, will refer to open circuit rms voltage. Under these conditions, the power transferred between units is $e_K^2/4R_s = e_K^2/1$ watts.

Beginning at the input mixer, the signal designated as $E_s(\omega_c)$ and the broadband noise $\sqrt{\eta}$ rms V/Hz are multiplied by the VCO input, with frequency $\omega_c - \omega_R$. The multiplication produces a replica of the signal at the sum and difference frequencies ω_R and $2\omega_c - \omega_R$. The multiplication process does not alter the uniform noise power density, i.e., the noise remains broad band at the output of the mixer (Reference 2). After multiplication, the output of the mixer is

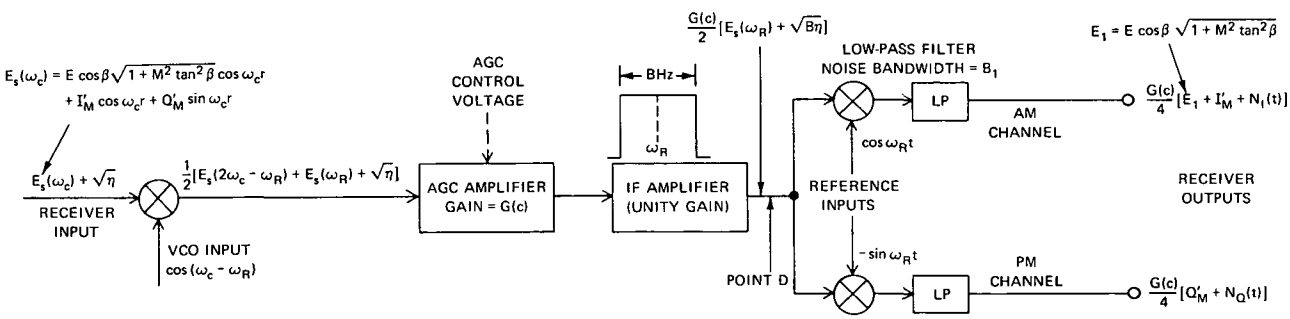

(A) Receiver equivalent circuit.

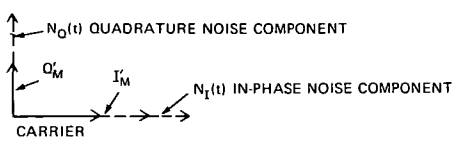

(B) Phasor diagram of signal at point D; $G(c)$ = 1.

Figure 19—Receiver equivalent circuit and phasor diagram.

$$\frac{1}{2}[E_s(\omega_R) + E_s(2\omega_c - \omega_R) + \sqrt{\eta}] . \tag{24}$$

The voltage represented by the above expression is applied to the broadband amplifier with gain $G(c)$ and then to the IF amplifier. The IF amplifier has a center frequency of ω_R and a noise bandwidth B; consequently, the signal term $E_s(2\omega_c - \omega_R)$ is eliminated. The output voltage of the IF is

$$\frac{G(c)}{2}[E_s(\omega_R) + \sqrt{\eta B}] . \tag{25}$$

The IF bandwidth is assumed to be sufficiently wide so as to pass the signal $E_s(\omega_R)$ without attenuation of the sideband structure (Part B of Figure 12). Now, the signal $E_s(\omega_R)$ at the IF output is the input signal

$$E[1 + ML(t)] \cos [\omega_c t + \beta L(t)]$$

translated to the intermediate frequency ω_R. This signal has been previously expressed in terms of in-phase and quadrature modulation components in Equation 19. Using this expansion, and letting $\omega_c = \omega_R$, gives the signal term at the IF output as

$$\frac{G(c)}{2}(E_c \cos \omega_R t + Q'_M \cos \omega_R t - I'_M \sin \omega_R t) , \tag{26}$$

where

$$E_c = E \cos\beta \sqrt{1 + M^2 \tan^2 \beta},$$

$$Q'_M = \frac{E(\sin\beta)(1 - M^2)}{\sqrt{1 + M^2 \tan^2 \beta}} L(t),$$

$$I'_M = \frac{EM}{\cos\beta \sqrt{1 + M^2 \tan^2 \beta}} L(t).$$

If the IF bandwidth B is small compared to the IF center frequency ω_R, the noise output will be narrowband Gaussian noise. Narrowband Gaussian noise can be resolved into two uncorrelated components $n_I(t)$ and $n_Q(t)$ as follows (Reference 3):

$$n_T(t) = n_I(t) \cos \omega_R t - n_Q(t) \sin \omega_R t , \tag{27}$$

where

$n_T(t)$ = total Gaussian noise voltage with frequency components from $\omega_R - B/2$ to $\omega_R + B/2$ Hz,

$n_I(t)$ = in-phase Gaussian noise voltage with frequency components from 0 to $B/2$ Hz,

$n_Q(t)$ = quadrature Gaussian noise voltage with frequency components from 0 to $B/2$ Hz.

The following relationship in terms of average power pertains, where N_I^2, N_Q^2, and N_T^2 are the powers corresponding to $n_I(t)$, $n_Q(t)$, and $n_T(t)$, respectively:

$$N_I^2 = N_Q^2 = \frac{1}{2}N_T^2 .$$

The IF output rms noise voltage from Equation 25 is $[G(c)/2]\sqrt{\eta B}$, and the power, therefore, is $[G^2(c)/4]\eta B$; hence,

$$N_T^2 = \frac{G^2(c)}{4}\eta B . \tag{28}$$

Because the signal and noise voltages both are expressed in terms of quadrature and in-phase components, they can be added to give a single expression: Adding Equation 26 to Equation 27 gives the IF output voltage as

$$\frac{G(c)}{2}\left\{E_c \cos \omega_R t + [n_I(t) + I'_M] \cos \omega_R t - [n_Q(t) + Q'_M] \sin \omega_R t\right\}. \tag{29}$$

The phasor plot of this equation is shown as Part B of Figure 19. The plot is identical with the plot shown by Part D of Figure 13 except that it includes the noise components $n_Q(t)$ and $n_I(t)$, and the reference phasor on the real axis is $\cos \omega_R t$ rather than $\cos \omega_c t$.

The IF output as given in Equation 29 is applied to the AM detector, where it is multiplied by the reference input $\cos \omega_R t$. The useful output, after removing terms in $2\omega_R$ in the low-pass filter following the detector, is the in-phase components of the input signal:

$$\text{AM output} = \frac{G(c)}{4}[E_c + I'_M + n_I(t)] . \tag{30}$$

The IF output is simultaneously applied to the PM detector where it is multiplied by the reference input, $-\sin \omega_R t$; the useful output is the quadrature components of the input signal:

$$\text{PM output} = \frac{G(c)}{4}[Q'_M + n_Q(t)] . \tag{31}$$

The S/N power ratio at the PM output is the ratio of the square of the signal voltage to the square of the rms value of the noise. From Equation 21, noting that N_Q is the rms value of $n_Q(t)$, we get

$$\text{S/N ratio (PM channel)} = \frac{(Q'_M)^2}{N_Q^2} = \frac{2(Q'_M)^2}{N_T^2} , \tag{32}$$

since $N_Q^2 = \frac{1}{2}N_T^2$. This latter relationship shows that only half of the noise power present at the input of the detector actually appears at the output—one of the prime advantages of a synchronous detector. Note that system gain $G(c)$ does not affect the S/N ratio.

Since the noise terms $n_I(t)$ and $n_Q(t)$ (Equations 30 and 31) occupy a bandwidth from 0 to $B/2$ Hz, it is necessary to modify the S/N ratio as given in Equation 32 if the PM detector is *followed* by a filter with a noise bandwidth less than $B/2$. For instance, if the post-detection filter noise bandwidth

is B_1, where $B_1 < B/2$, the noise power term, N_Q^2 in Equation 32, must be modified by the factor $B_1/(B/2)$, or $2B_1/B$. In this case,

$$\begin{matrix}\text{S/N ratio (PM channel)} \\ \text{with post-detection filtering}\end{matrix} = 2\frac{(Q'_M)^2}{N_T^2}\frac{B}{2B_1}, \quad \text{when } B_1 < \frac{B}{2} \tag{33}$$

where B is the noise bandwidth at IF and B_1 is the noise bandwidth post-detection filter. Since the purpose of this section is to show the effect of incidental AM on the output S/N ratio of the PM channel, the S/N ratio will be compared to the S/N ratio when AM is not present, i.e., $M = 0$. The relative S/N ratio for this purpose will be defined by

$$\begin{matrix}\text{Relative S/N ratio} \\ \text{(PM channel)}\end{matrix} = \frac{\text{S/N}}{\text{S/N } (M = 0)}.$$

Substituting the PM channel S/N ratio with post-detection filtering as given in Equation 33 results in

$$\begin{aligned}\begin{matrix}\text{Relative S/N ratio} \\ \text{(PM channel)}\end{matrix} &= 2\frac{(Q'_M)^2}{N_T^2}\frac{B}{2B_1}\Bigg/2\frac{(Q'_{M(M=0)})^2}{N_T^2}\frac{B}{2B_1} \\ &= \left(\frac{Q'_M}{Q'_{M(M=0)}}\right)^2 \end{aligned} \tag{34}$$

Note that post-detection filtering does not affect the relative S/N ratio as defined above. To evaluate, we use Q'_M as defined below Equation 25. Also, $Q'_{M(M=0)} = E(\sin\beta)L(t)$. Substitution into the above relationship gives

$$\begin{matrix}\text{Relative S/N ratio} \\ \text{(PM channel)}\end{matrix} = \left(\frac{1 - M^2}{\sqrt{1 + M^2\tan^2\beta}}\right)^2, \text{ in terms of dB,}$$

$$= 20\log\frac{1 - M^2}{\sqrt{1 + M^2\tan^2\beta}}. \tag{35}$$

This relationship has been plotted in Figure 20 for $\beta = 57.52$ deg (Curve 1) and $\beta = 70$ deg (Curve 2), with the dB scale as the ordinate and M in percent as the abscissa. The plotted data show that in-phase incidental AM reduces the S/N ratio and that as β is *increased*, the percentage of AM which is tolerable is *reduced*. For instance, if a 1 dB S/N reduction is accepted, then M can have a maximum value of 23 percent if $\beta = 57.52$ deg and 16 percent if $\beta = 70$ deg; other values computed from Equation 10 are maximum $M = 30$ percent if $\beta = 38$ deg and maximum $M = 4.4$ percent if $\beta = 85$ deg.

Ordinarily, only the PM channel of the receiver is utilized for extracting demodulated data; the present design does not permit the use of both channels simultaneously because only a single output amplifier, which is switched to either the PM of the AM detector, is provided. However, if incidental AM is present to any degree in the input signal, it would seem advantageous to utilize both channels since the demodulated wave form $L(t)$ appears simultaneously in both channels in phase coincidence,

or in phase opposition. The choice as to utilizing both channels would depend upon whether summing improved the S/N ratio compared with the S/N ratio of the PM channel. The simplest method for determining the possible improvement is to compare the S/N ratio of the summed channels with the PM channel S/N ratio when $M = 0$, the same reference used in deriving Equation 35. The improvement in dB will then appear as the difference in dB between a plot of the summed S/N and the previous plot of Equation 35. Accordingly, the relative S/N ratio of the sum of both channels is defined as

$$\frac{\text{Signal power (sum)}}{\text{Noise power (sum)}} \div \frac{\text{PM channel signal power } (M = 0)}{\text{PM channel noise power}} .$$

The total signal voltage if both channels are summed in the proper phase is

$$I'_M + Q'_M = \frac{M + \cos\beta\,(\sin\beta)(1 - M^2)}{\cos\beta\sqrt{1 + \tan^2\beta}} L(t) ,$$

from the definitions of I'_M and Q'_M as given below Equation 26. The total signal power is the square of this term, since the average power in a square wave is the square of its peak amplitude. The noise power in the PM and AM channels with post-detection filtering with bandwidth B_1 Hz, where $B_1 < B/2$, is $(2B_1/B)N_Q^2$ and $(2B_1/B)N_I^2$, respectively. Consequently,

$$\text{Relative S/N ratio (sum of both channels)} = \frac{(I'_M + Q'_M)^2}{(2B_1/B)(N_Q^2 + N_I^2)} \Bigg/ \frac{(Q'_{M(M=0)})^2}{(2B_1/B)N_Q^2}$$

$$= \frac{(I'_M + Q'_M)^2}{(Q'_{M(M=0)})^2} \frac{N_Q^2}{N_I^2 + N_Q^2} ,$$

but $N_Q^2 + N_I^2 = N_T^2$ and $N_Q^2 = \frac{1}{2}N_T^2$, so the relative S/N ratio reduces to $(I'_M + Q'_M)^2/2(Q'_{M(M=0)})^2$, which again is independent of post-detection filtering. Evaluation using the value of $I'_M + Q'_M$ given above, as well as the relationship $Q'_{M(M=0)} = EL(t)\sin\beta$, gives

$$\text{Relative S/N ratio (summed channels) (dB)} = 20 \log \left[\frac{M + \cos\beta(\sin\beta)(1 - M^2)}{\sqrt{2}\sin\beta\,(\cos\beta)\sqrt{1 + M^2\tan^2\beta}} \right] . \quad (36)$$

This relationship is plotted in Figure 20 as Curves 3 and 4, corresponding to $\beta = 57.52$ deg and $\beta = 70$ deg, respectively. Comparison of each of these curves with the S/N ratio of the PM channel having the same value of β shows that there is a range of M from zero to the crossover point for which the

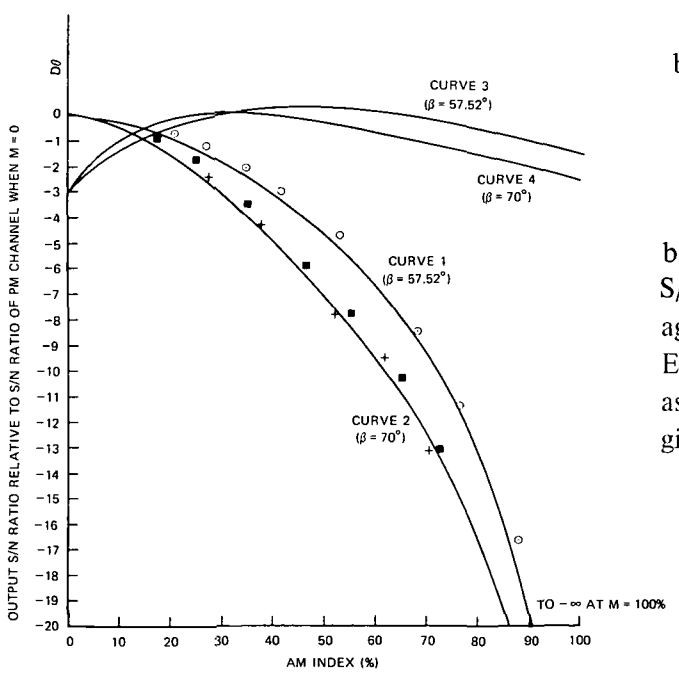

Figure 20—Effect of in-phase incidental AM on S/N power ratio of receiver outputs for the PM channel only (Curves 1 and 2) and the sum of the AM and PM channels (Curves 3 and 4). The measured data points are shown by the symbols; the theoretical predictions are shown by the curves.

S/N of the PM channel is superior to the summed channels. Beyond the value of M corresponding to the crossover point where the S/N ratios are equal, the summed channel offers an increasing improvement in the S/N ratio. The value of M corresponding to the crossover point decreases for the higher values of β: If $\beta = 38$ deg, the crossover point occurs for $M = 19$ percent; if $\beta = 57.52$ deg, $M = 18$ percent; if $\beta = 70$ deg, $M = 13$ percent; if $\beta = 85$ deg, $M = 3.6$ percent.

This section will conclude with a discussion of the measured S/N power ratio of the PM channel made to determine the validity of Equation 35. The data points for these measurements are plotted as circles for Curve 1 (Figure 20) and crosses and squares for Curve 2. Each set of points is a measurement made for a different value of the reference S/N ratio (the PM channel S/N ratio, for $M = 0$). The data shown as circles (Curve 1) are a measurement of the PM channel S/N ratio versus M, referred to a reference S/N ratio (for $M = 0$) of 18 dB. The crosses (Curve 2) were measured with an initial S/N ratio of 16 dB; for the squares (Curve 2), the S/N ratio (for $M = 0$) was set at 3.3 dB. For these measurements, the fundamental frequency of the square-wave modulation wave form $L(t)$ was 3 kHz; the post-detection filter noise bandwidth was 60 kHz. This latter was set so as to pass $L(t)$ with an essentially unaltered rise time.

The last series of measurements, with an initial S/N ratio (for $M = 0$) of 3.3 dB, provides a good test of the predicted S/N ratio under marginal conditions, in that a S/N ratio this low would not yield useable data in most cases. In this case, the reasonably good fit with the theory indicates that the AGC and VCO loops of the receiver were relatively unaffected by the noise, since the theory assumes zero loop errors for both servos. The noise power in the loops is, of course, much less than the noise in the data channel because the noise bandwidths of the loops are relatively small. In the case of the VCO loop, the noise bandwidth employed in taking the data was set on the front panel of the receiver, at 30 Hz. If the noise power density at the output of the PM detector is η_o W/Hz, the noise power in the loop is $30 \times \eta_o$ W. To demodulate the 3-kHz square wave, the post-filter bandwidth was required to be set such that the equivalent noise bandwidth was 60 kHz with a consequent noise power of $60 \times 10^3 \times \eta_o$ W. The loop noise power is, consequently, 33 dB below the data noise power, $-33 = 10 \log [30/(60 \times 10^3)]$, assuming that the PM detector performs the dual function of demodulation and simultaneously provides an error signal to the VCO loop filter. The noise power in the AGC loop was estimated to be of the order of 30 dB below the data noise power. The accuracy of this figure is uncertain since the AGC receiver adjustment is calibrated in terms of a time constant rather than noise bandwidth. It was calculated that the 0.3-s time-constant setting selected in taking the data had a noise bandwidth of 50 to 100 Hz, assuming the AGC filter characteristic to be that of an RC integrator.

The performance of the loops is also affected by the signal carrier power, or more specifically, the carrier-to-loop noise power. With regard to loop performance, incidental AM is in a sense beneficial since it increases the carrier power. For instance, according the carrier term $E \cos\beta\sqrt{1 + M^2 \tan^2\beta}$ (Equation 26), if $M = 100$ percent and $\beta = 70$ deg, the carrier power increases 9.3 dB relative to the value when $M = 0$ (pure PM).

It was concluded that the principal undesirable effect of in-phase incidental AM is the resulting S/N reduction of the PM channel output.

Effect of Incidental In-Phase AM on Signal Power Division

An important consideration from the systems aspect of the operation of phase-modulated transmitters is the partition of signal power between the carrier and modulation components. In the case of pure square-wave PM, the division of power will depend only on the PM index β. However, if incidental AM is present, the partition will also depend upon the AM index M. The partition process is usually described by the two power ratios P_c/P_t and P_M/P_t, where P_c is the signal carrier power, P_M is the power in the modulation component, and P_t is the total signal power. For pure square-wave phase modulation, the term P_M will consist only of components in quadrature with the carrier, as shown in the phasor diagram in Part A of Figure 8. However, if incidental AM is present, P_M will contain in-phase modulation power in addition to quadrature modulation power. Since the in-phase and quadrature components are separated in the receiver demodulation process, the two components will be treated separately by deriving the ratios P_{QM}/P_t and P_{IM}/P_t, where P_{QM} is the power in the signal quadrature modulation components and P_{IM} is the power in the in-phase modulation components.

The derivation of the signal power division can be obtained most conveniently from Equation 19, which is the expression describing the phasor representation shown in Part D of Figure 13. For the present use, we replace the term $(1 + M^2 \tan^2 \beta)^{1/2}$ with its equivalent $(\cos^2 \beta + M^2 \sin^2 \beta)^{1/2} \times (\cos \beta)^{-1}$; the signal expression representing a PM signal with in-phase incidental AM can then be written

$$E_{\text{signal}} = E(\cos^2 \beta + M^2 \sin^2 \beta)^{1/2} \cos \omega_c t + I'_M \cos \omega_c t - Q'_M \sin \omega_c t \,, \tag{37}$$

where

$$I'_M = \frac{EML(t)}{(\cos^2 \beta + M^2 \sin^2 \beta)^{1/2}} \tag{38}$$

$$Q'_M = \frac{E \sin \beta \, (\cos \beta)(1 - M^2)L(t)}{(\cos^2 \beta + M^2 \sin^2 \beta)^{1/2}} . \tag{39}$$

The average power in the carrier component of Equation 37 is given by

$$P_c = \frac{E^2}{2}(\cos^2 \beta + M^2 \sin^2 \beta) \tag{40}$$

since the average power of a sine wave, $E \sin \omega t$, is $\frac{1}{2}E^2$. The average power represented by the quadrature modulation components is $\frac{1}{2}Q'^2_M$:

$$P_{QM} = \frac{E^2 \sin^2 \beta \, (\cos^2 \beta)(1 - M^2)^2}{2(\cos^2 \beta + M^2 \sin^2 \beta)} , \tag{41}$$

from Equation 39. The average power represented by the in-phase modulation components is $\frac{1}{2}I'^2_M$:

$$P_{IM} = \frac{E^2 M^2}{2(\cos^2 \beta + M^2 \sin^2 \beta)} , \tag{42}$$

from Equation 38. In Equations 41 and 42, note that $L^2(t) \equiv 1$ since $L(t)$ is a unit-amplitude square wave. The total power in the signal is given by

$$P_t = P_c + P_{QM} + P_{IM} ;$$

adding Equations 40, 41, and 42 gives

$$P_t = \frac{E^2}{2} \frac{\cos^2\beta\,(\sin^2\beta)(1 - M^2)^2 + M^2 + \cos^2\beta + M^2\sin^2\beta}{\cos^2\beta + M^2\sin^2\beta}$$

To reduce the above expression, we use the equivalent

$$\cos^2\beta + M^2\sin^2\beta \equiv 1 - \sin^2\beta\,(1 - M^2) ;$$

the expression will then simplify to

$$P_t = \frac{E^2}{2}(1 + M^2) . \tag{43}$$

The desired power relation P_c/P_t is found by dividing Equation 40 by Equation 43:

$$\frac{P_c}{P_t} = \frac{\cos^2\beta + M^2\sin^2\beta}{1 + M^2} . \tag{44}$$

The ratio of quadrature modulation power P_{QM} to total signal power is obtained by dividing Equation 41 by Equation 43:

$$\frac{P_{QM}}{P_t} = \frac{\sin^2\beta(\cos^2\beta)(1 - M^2)^2}{(\cos^2\beta + M^2\sin^2\beta)(1 + M^2)} . \tag{45}$$

The ratio of in-phase modulation power P_{IM} to total signal power is found by dividing Equation 42 by Equation 43:

$$\frac{P_{IM}}{P_t} = \frac{M^2}{(\cos^2\beta + M^2\sin^2\beta)(1 + M^2)} . \tag{46}$$

Figure 21 shows the ratio P_c/P_t in dB versus the PM index β for various fixed values of M. The curve that is highest on the left, intended as a reference, shows this ratio for pure PM ($M = 0$). A comparison with the reference curve shows that the general effect of incidental AM is to cause the P_c/P_t ratio to become more linear, finally becoming a horizontal line at -3 dB, when $M = 1$. (Note: The *signal* is converted to pure AM when $M = 1$, since $P_c = \frac{1}{2}E^2$, from Equation 40; $P_{IM} = \frac{1}{2}E^2$, from Equation 42; and $P_{QM} = 0$, from Equation 41, which is to say half the signal power resides in the carrier and half in the in-phase modulation content.) At $\beta = 45$ deg, incidental AM does not change P_c/P_t. Below 45 deg, incidental AM increases P_c/P_t; above 45 deg, incidental AM decreases P_c/P_t. The power division of the signal modulation components relative to the total power is shown in Figures 22 and 23. Figure 22 shows the in-phase modulation power division P_{IM}/P_t (Equation 46), while Figure 23 shows the quad-

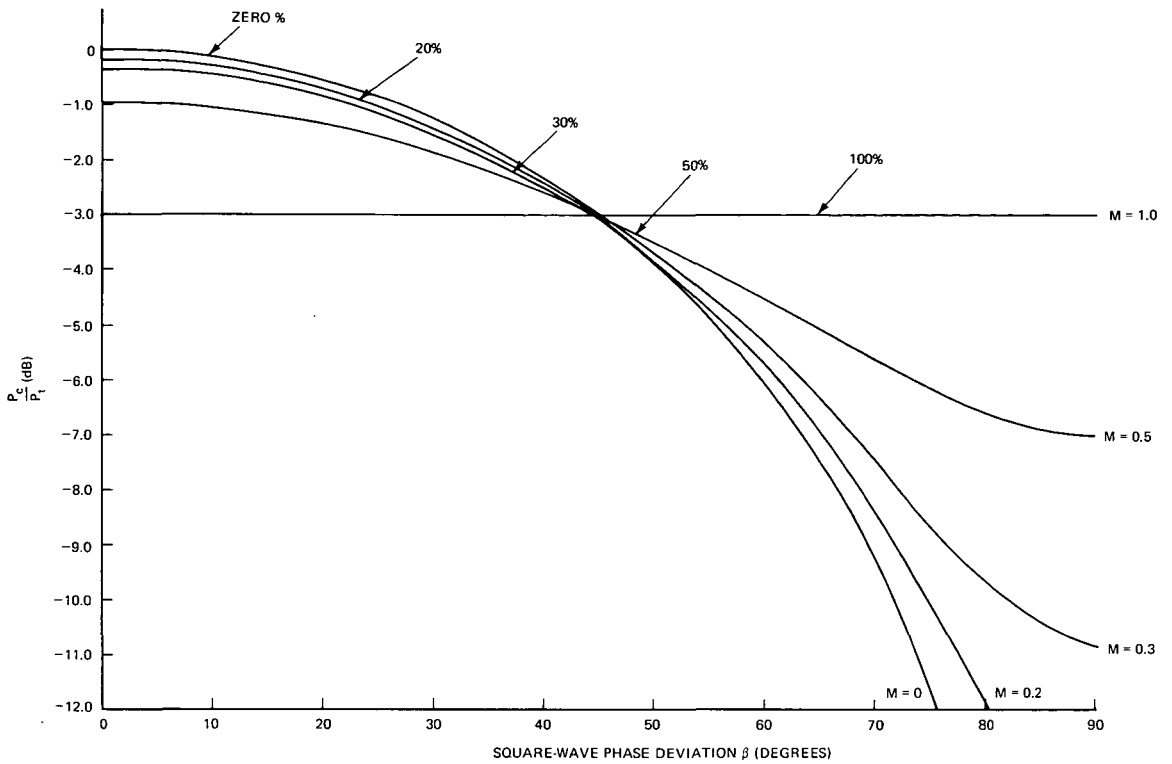

Figure 21—Ratio of carrier power to total signal power versus β for various percentages of incidental AM.

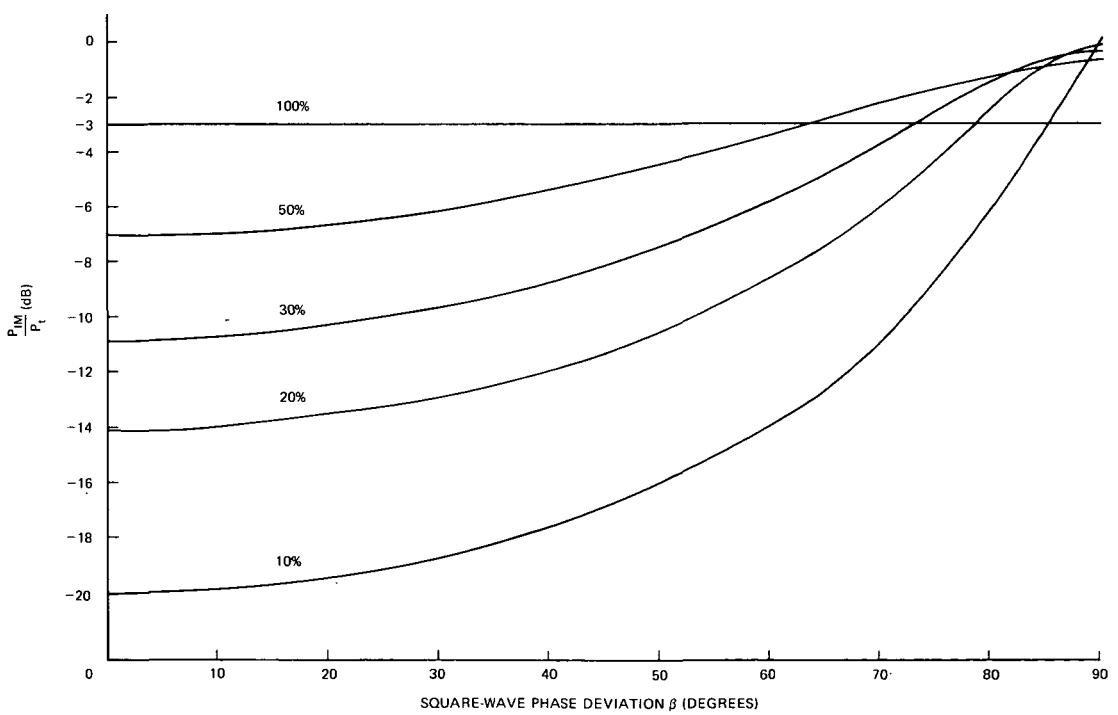

Figure 22—Ratio if in-phase modulation power to total signal power versus β for various percentages of incidental AM.

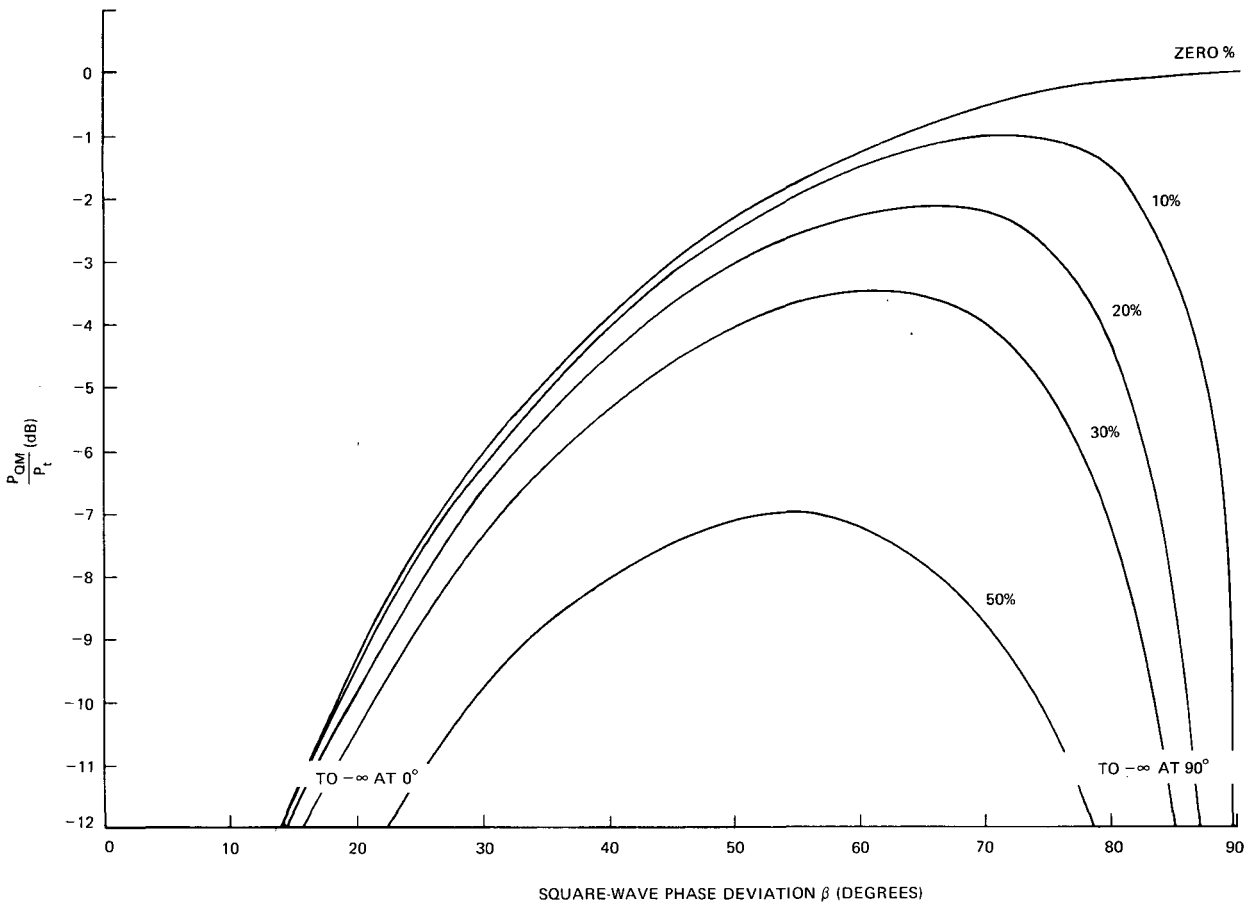

Figure 23—Ratio of quadrature modulation power to total signal power versus β for various percentages of incidental AM.

rature modulation power division P_{QM}/P_t (Equation 45). The two ratios are plotted in dB versus β for various values of the AM index M. An inspection of the modulation power division plotted in the two sets of Figures shows that the general effect of incidental AM is to reduce the quadrature modulation power and to increase the in-phase modulation power relative to the normal quadrature or modulation power in the absence of AM ($M = 0$). Further, the relative changes in the power division for a fixed percentage of AM increase as the PM index β increases. For example, if $\beta = 1$ rad, and $M = 0$ (normal square-wave PM), $P_{QM}/P_t = -1.5$ dB and $P_{IM}/P_t = -\infty$ dB. If M is increased from a value of zero to 20 percent, then $P_{QM}/P_t = -2.4$ dB, a reduction of 0.9 dB, and $P_{IM}/P_t = -9.1$ dB. If $\beta = 70$ deg, and $M = 0$, $P_{QM}/P_t = -0.55$ dB, while $P_{IM}/P_t = \infty$ dB as before. If M is increased to 20 percent, $P_{QM}/P_t = -2.2$ dB, a reduction of 1.65 dB, and $P_{IM}/P_t = -6$ dB.

Figure 21 shows the effect of AM on the carrier to be somewhat less than the effect on the modulation components. If $\beta = 1$ rad and $M = 0$ (normal PM), $P_c/P_t = -5.5$ dB; with an increase of M to 20 percent, $P_c/P_t = -5.2$ dB, an increase of 0.3 dB. If $\beta = 70$ deg and $M = 0$ (normal PM), $P_c/P_t = -9.3$ dB; with an increase of M to 20 percent, $P_c/P_t = -8.4$ dB, a change of + 0.9 dB.

CHAPTER 5

CONCLUSIONS

Satellite transmitters may produce some degree of unwanted AM which occurs synchronously as the transmitter is phase modulated. One source of incidental AM is an improperly terminated transmitter phase modulator. The object of this report has been to determine the level of AM which can be tolerated. The criterion adopted for determining the level of tolerance is the effect incidental AM produces on the output S/N power ratio of the phase-lock receiver used to demodulate the signal. The analysis presented in this report has been limited to a periodic square-wave modulating signal and the receiver to a type which does not employ a limiter preceding the phase detector supplying the error signal to the VCO; this type of receiver (Electrac Model 215) was used in taking data to verify the analysis.

Measurements show the most probable type of incidental AM likely in a satellite transmitter is synchronous AM in phase coincidence or in phase opposition with respect to the PM content of the signal, i.e., a signal of the form

$$E[1 \mp ML(t)] \cos [\omega_c t + \beta L(t)] ,$$

where

M = AM index ($0 \leqslant M \leqslant 1$),

β = PM index in radians,

$L(t)$ = unit peak amplitude square wave,

ω_c = carrier frequency.

The following conclusions pertain to this type of signal:

1. The presence of in-phase incidental AM causes a reduction in the S/N ratio at the receiver PM channel output. Relatively large percentages of incidental AM are required to produce a significant reduction. For example, if the output S/N is sufficiently above the data threshold so that a 1-dB reduction is acceptable when the peak PM index is 1 rad, then a maximum level of 23-percent AM ($M = 0.23$) is tolerable. If the PM index is 1.22 rad (70 deg), then 16-percent AM is tolerable. The tolerable level of AM is further reduced for larger values of β, e.g., 4 percent if $\beta = 1.5$ rad.

2. Although the S/N ratio of the PM channel is adversely affected as noted, the adverse effect can be mitigated by summing both the AM and PM channels of the receiver. There will be an improvement in the S/N of the summed channels only if the level of AM is greater than 15 percent.

3. In-phase incidental AM alters the normal balance of power between the carrier and modulation content of the signal. Normal balance means the proportions characteristic of a pure square-wave phase-modulated signal. For example, if $\beta = 1$ rad, 20-percent superimposed AM will cause the carrier-to-total power ratio P_c/P_t to increase by 0.3 dB and the quadrature modulation power-to-total power ratio P_{QM}/P_t to decrease by 0.9 dB; the in-phase modulation-to-total power ratio P_{IM}/P_t will assume a value of -9.2 dB. (Normal square-wave PM has zero in-phase modulation content.) The changes are larger for higher values of β: If $\beta = 70$ deg, 20-percent superimposed AM causes P_c/P_t to increase by 0.9 dB, P_{QM}/P_t to decrease by 1.6 dB, and P_{IM}/P_t to assume a value of -6 dB.

4. In-phase incidental AM alters the spectral amplitudes of a normal PM signal but not the symmetry; both normal PM and PM with superimposed AM have symmetrical spectrums. Spectral analysis is not an ideal method for testing a transmitter for AM. Viewing the envelope or demodulating the signal in a phase-lock receiver is preferred. Even very small percentages of AM can be detected by observing the AM channel output. Incidental AM will cause a square-wave output; pure square-wave PM will show zero output.

If the superimposed synchronous AM is shifted in time so as to be in quadrature, i.e., the signal is of the form

$$E[1 \pm ML(t + P/4)] \cos [\omega_c t + \beta L(t)] \ ,$$

where P is the period of $L(t)$, the signal spectrum becomes asymmetrical. The presence of incidental AM in this case can easily be detected by spectral analysis. The S/N of the receiver output is not changed by this type of AM; the principal effect is the generation of a double frequency square wave which is superimposed on the normal PM channel output of the receiver.

Goddard Space Flight Center
National Aeronautics and Space Administration
Greenbelt, Maryland, March 2, 1971
861-41-75-01-51

REFERENCES

1. Rogers, L. J., and Hepler, D. S., "Constant Amplitude Variable Phase Filters", NASA Technical Note D-2758, May 1965.

2. Tausworthe, R. C., "Theory and Practical Design of Phase Locked Receivers", Technical Report No. 32-819, Vol. I, pp. 64-65, Jet Propulsion Laboratory, California Institute of Technology, February 1966.

3. Davenport, W. B., Jr., and Root, W. L., "An Introduction to the Theory of Signals and Noise", pp. 150-165, McGraw-Hill Book Co., New York, 1958.

Appendix A

Phase-Lock Demodulator

Figure A.1 shows the basic components of a heterodyne phase-lock demodulator of a type having coherent AGC but not containing a limiter. The input signal is applied to the first mixer, where it is heterodyned with an input from the VCO. The resulting sum and difference terms are fed to the IF amplifier, where one of the set is selectively amplified and fed simultaneously to the quadrature and main, or loop, phase detector. The loop phase detector compares the phase of the incoming signal with that of the reference oscillator and develops an error voltage which is fed to the loop filter and then to the VCO; the oscillator assumes a phase angle such as to minimize the loop error. If PM is present in the input signal and the modulating frequency is sufficently greater than the loop bandwidth, the demodulated signal will appear at the output of the main phase detector.

Signal gain within the receiver is established by a second loop which controls the gain of the IF amplifier so as to maintain a constant carrier level: The signal input to the synchronous detector is multiplied by an in-phase signal from the reference oscillator, which produces a signal proportional to the carrier level. This signal is, in turn, filtered by the AGC filter and is fed to a subtractor, where it is

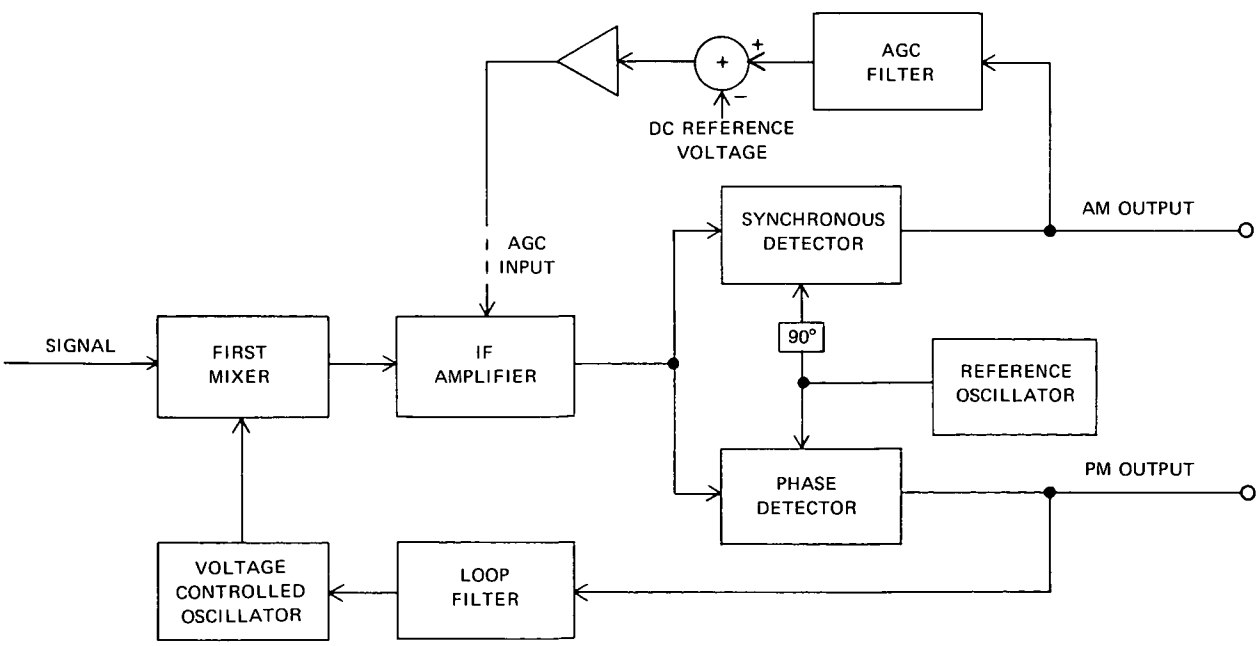

Figure A.1—Phase-lock demodulator block diagram.

compared to a fixed reference voltage; the resulting difference, or error, voltage is amplified and used to control the IF gain. If the signal is amplitude modulated, in-phase components of the signal will appear at the output of the synchronous detector, provided that the AGC time constant is greater than the period of the modulating signal.

For the purpose of analyzing the demodulation process, the receiver block diagram, Figure A.1, is replaced by the equivalent circuit shown in Figure A.2. In the equivalent circuit, the input mixer and the detectors are represented as multipliers. Principal parameters involved in the analysis are tabulated in Table A.1: Part A shows the required input signal form; Part B shows the principal receiver parameters; and Part C shows the parameters involved to define the steady-state operation. The basic method followed in the analysis follows: (1) The receiver input signal is written in I and Q form as shown in Part A of Table A.1. (2) We assume the receiver to be initially in frequency synchronism but not in phase lock. (3) With frequency synchronism, the receiver outputs are calculated using the equivalent circuit, Figure A.2. This leads to an output expression in terms of the input factors I and Q, the receiver IF gain $G(c)$, and the VCO phase-injection angle ϕ. (4) The dependent variables $G(c)$ and ϕ can be evaluated by invoking two steady-state conditions which exist when the receiver is in phase lock: the dc error voltages in the VCO loop and AGC loop are zero. With these latter conditions, the desired output is obtained in terms of I and Q only. The use of the equivalent circuit to determine the receiver outputs when the input is a modulated signal is given in Case I of the text and will not be repeated; instead, the relationship of the equivalent circuit to more basic theory will be treated briefly.

In the literature,* the basic phase-locked loop is represented as shown in Figure A.3, where the phase detector is modeled as a subtractor followed by a device which takes the sine of the phase difference function $\theta_i(t) - \phi(t)$, where $\theta_i(t)$ is the phase of the input signal and $\phi(t)$ is the phase of the VCO input to the subtractor. Phase lock is defined as the steady-state condition when $\theta_i(t) - \phi(t) = 0$.

Table A.1—Principal parameters involved in equivalent circuit of demodulator.

(A) Input Signal Form	(B) Receiver Parameters	(C) Receiver Parameters Used to Define Steady-State Operation
$I \cos \omega_c t - Q \sin \omega_c t$	ϕ = VCO phase angle	$\Delta\epsilon_{AGC}$ = AGC error voltage
I = factor preceding in-phase carrier component $\cos \omega_c t$	$G(c)$ = IF variable gain parameter	$\Delta\epsilon_{loop}$ = loop error voltage
Q = factor preceding quadrature carrier component $\sin \omega_c t$	ω_R = radian frequency of reference	
ω_c = radian carrier frequency	K_R = AGC reference voltage	

*Viterbi, A. J., "Principles of Coherent Communication", pp. 10-17, McGraw-Hill Book Co., New York, 1966.

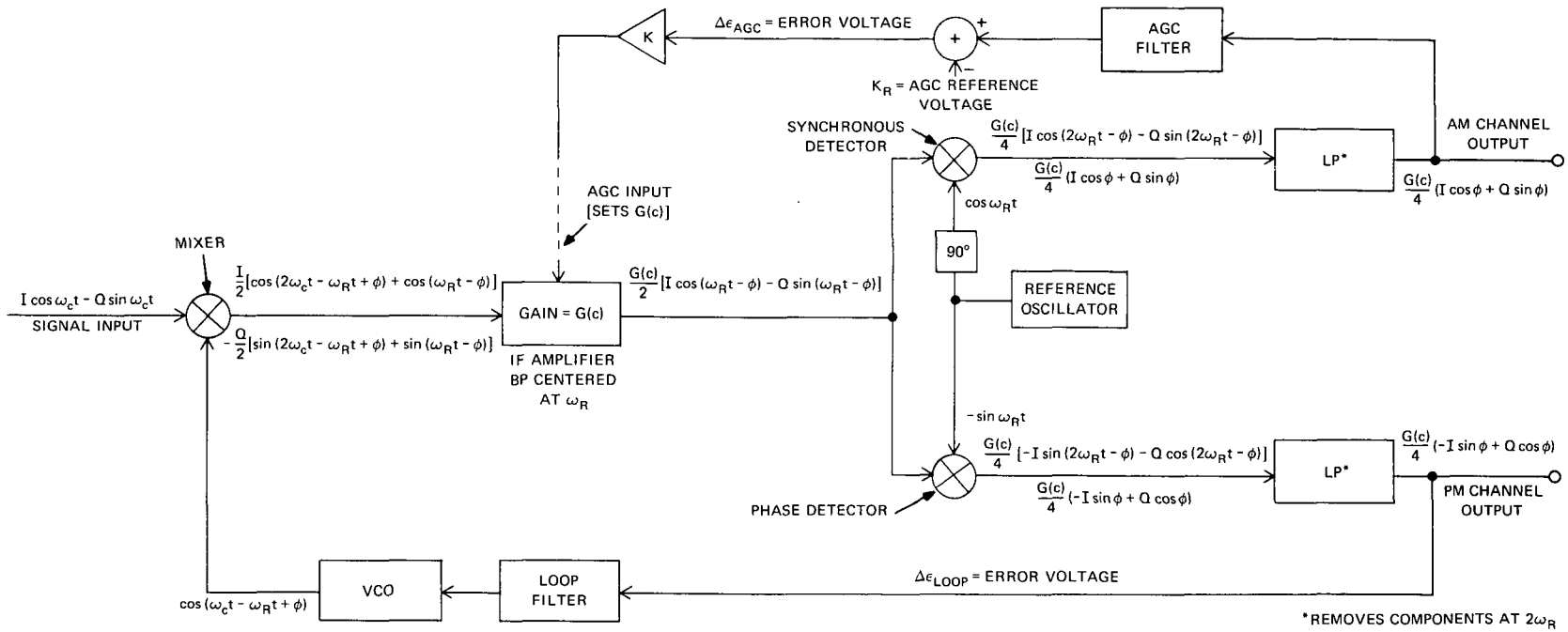

Figure A.2—Phase-lock demodulator equivalent circuit showing signal path.

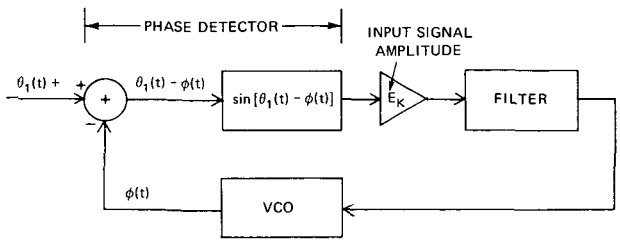

Figure A.3—Basic phased-locked loop system.

Given $\theta_i(t)$, the dynamic process whereby $\phi(t)$ is determined is a complicated method which requires the solution of a nonlinear differential equation (nonlinear because of the sine operator in the loop). The heterodyne demodulator diagramed in Figure A.2 can be reduced to the basic configuration shown in Figure A.3, although use of the input signal in the I and Q form differs from that shown in the literature. To show that the I and Q form of input signal results in a loop phase detector output of the classic form $\sin[\theta_i(t) - \phi(t)]$, we consider an unmodulated input signal:

$$E\cos(\omega_c t + \theta_i) = E(\cos\omega_c t\cos\theta_i - \sin\omega_c t\sin\theta_i)\,,$$

where ω_c is the carrier frequency and θ_i is the initial phase angle. Then, from the definitions given in Part A of Table A.1,

$$\begin{aligned} I &= E\cos\theta_i\,, \\ Q &= E\sin\theta_i\,. \end{aligned} \tag{A.1}$$

Letting the VCO frequency be $\omega_c - \omega_R + \phi$ results in the input frequency to the phase detectors being equal to the reference frequency: The output of the input multiplier will be the sum and difference frequency terms:

$$\frac{E\cos\theta_i}{2}[\cos(2\omega_c t - \omega_R t + \phi) + \cos(\omega_R t - \phi)]$$

$$-\frac{E\sin\theta_i}{2}[\sin(2\omega_c t - \omega_R t + \phi) + \sin(\omega_R t - \phi)]\,.$$

The IF amplifier with bandpass at ω_R will pass only the ω_R terms with a gain of $G(c)$. The output of the IF amplifier is, consequently,

$$\frac{EG(c)}{2}[\cos\theta_i\cos(\omega_R t - \phi) - \sin\theta_i\sin(\omega_R t - \phi)]\,. \tag{A.2}$$

At the loop phase detector, this signal is multiplied by the reference signal $-\sin\omega_R t$; terms in $2\omega_R t$ are filtered out. The loop phase detector output is the term

$$\frac{EG(c)}{4}(-\cos\theta_i\sin\phi + \sin\theta_i\cos\phi) = \frac{EG(c)}{4}(-I\sin\phi + Q\cos\phi)\,;$$

the equality follows from the definitions of I and Q (Equation A.1). The first term above reduces to $EG(c)/4\sin(\theta_i - \phi)$ according to the identity for $\sin(A - B)$. This term is the error input to the VCO:

$$\frac{EG(c)}{4} \sin(\theta_i - \phi) = \Delta\epsilon_{\text{loop}} . \tag{A.3}$$

Equation A.3 is seen to be identical to the classic form of the phase detector (Figure A.3); note that in this case $\theta_i(t) = \theta_i$ and $\phi(t) = \phi$. According to theory, the loop phase error at $t = -\infty$ (steady-state error) will be zero when phase lock is achieved if (1) the loop is of second order (i.e., the loop filter contains a perfect integrator) and the carrier frequency does not change with time after lock is achieved or (2) the loop is of third order (i.e., the loop contains two perfect integrators) and the carrier frequency is either constant or changes linearly with time. It will be assumed that the loop is of a least second order and that lock has been achieved. Consequently,

$$\begin{aligned} \frac{EG(c)}{4} \sin(\theta_i - \phi) &= \Delta\epsilon_{\text{loop}} \\ &= 0 , \end{aligned} \tag{A.4}$$

so that $\theta_i - \phi = n\pi$, where $n = 1, 2, 3, \ldots$. However, odd multiples of π are not stable points of lock*; therefore,

$$\theta_i - \phi = 0 , \quad \text{or} \quad \theta_i = \phi . \tag{A.5}$$

Equation A.5 eliminates the dependent variable ϕ. To eliminate the remaining dependent variable $G(c)$, we calculate the AM channel output: The synchronous detector AM output is the input signal Equation A.2 multiplied by the reference input $\cos \omega_R t$. After filtering terms in $2\omega_R t$, this product is

$$\frac{EG(c)}{4} (\cos\theta_i \cos\phi + \sin\theta_i \sin\phi) = \frac{G(c)}{4} (I \cos\phi + Q \sin\phi) ,$$

from the definitions of I and Q (Equation A.1). However, from Equation A.5, $\theta_i = \phi$, and $\sin^2 A + \cos^2 A \equiv 1$; consequently, the output reduces to

$$\frac{EG(c)}{4} = \text{synchronous detector output} . \tag{A.6}$$

This dc term is applied to the AGC subtractor and compared with K_R, the AGC reference voltage (Figure A.2). The difference is the error voltage $\Delta\epsilon_{\text{AGC}}$:

$$\Delta\epsilon_{\text{AGC}} = \frac{EG(c)}{4} - K_R . \tag{A.7}$$

It will be assumed that the AGC gain is infinite so that $\Delta\epsilon_{\text{AGC}} = 0$; thus, from Equation A.7,

$$\frac{EG(c)}{4} = K_R \quad \text{and} \quad G(c) = \frac{4K_R}{E} . \tag{A.8}$$

*Viterbi, A. J., "Principles of Coherent Communication", pp. 44-50, McGraw-Hill Book Co., New York, 1966.

Finally, substitution of $G(c)$ into Equation A.5 gives

$$\text{AM channel output} = K_R \,. \tag{A.9}$$

Substitution of the value for $G(c)$ into Equation A.4 gives the PM output as

$$\begin{aligned} K_R(\sin \phi_i - \phi) &= \Delta\epsilon \\ &= 0 \,. \end{aligned} \tag{A.10}$$

The factor K_R which results in Equation A.10 illustrates an important characteristic of the use of correlated AGC, namely, that the bandwidth of the VCO loop after lock is achieved becomes independent of input signal level. Note that in the basic model (Figure A.3), the loop gain is affected by the input signal level since the input signal level amplitude E_K appears in the feed back path. The constancy of loop bandwidth in a phase-lock circuit pertains only if a limiter is *not* employed preceding the phase detector since in the presence of noise, the limiter reduces the loop gain. In general, second-order loops employ limiters, whereas third-order loops (utilized in the Model-205 demodulator discussed in the text) do not, presumably because the more difficult stability constraints require a constant loop gain.

Appendix B

Signal Expression and Spectrum of a Square-Wave PM Signal

Signal Expression

A carrier, $E \cos \omega_c t$, phase modulated at a level of β peak radians by a square wave can be written as

$$E \cos [\omega_c t + \beta L(t)] ,$$

where $L(t)$ is the symmetrical square wave with a period P, expressable in the interval $0 < t < P$ as

$$L(t) = \begin{cases} 1, & \text{for } 0 < t < \frac{P}{2} \\ -1, & \text{for } \frac{P}{2} < t < P \end{cases}$$

and β is the PM index in radians. To determine the signal expression, we expand Equation B.1 with the identity $\cos (A + B) \equiv \cos A \cos B - \sin A \sin B$:

$$E \cos [\omega_c t + \beta L(t)] = E \cos \omega_c t \cos [\beta L(t)] - \sin \omega_c t \sin [\beta L(t)] . \tag{B.1}$$

According to the definition of $L(t)$, it follows that

$$\cos [\beta L(t)] = \begin{cases} \cos \beta, & \text{for } 0 < t < \frac{P}{2} \\ \cos (-\beta), & \text{for } \frac{P}{2} < t < P \\ \cos \beta, & \ldots\ldots \end{cases}$$

but $\cos (-\beta) \equiv \cos (\beta)$; consequently,

$$\cos [\beta L(t)] \equiv \cos \beta . \tag{B.2}$$

Now,

$$\sin[\beta L(t)] = \begin{cases} \sin\beta, & \text{for } 0 < t < \frac{P}{2} \\ \sin(-\beta), & \text{for } \frac{P}{2} < t < P \\ \sin\beta, & \ldots\ldots \end{cases}$$

but $\sin(-\beta) \equiv -\sin\beta$; thus,

$$\sin[\beta L(t)] = \begin{cases} +1\sin\beta, & \text{for } 0 < t < \frac{P}{2} \\ -1\sin\beta, & \text{for } \frac{P}{2} < t < P \\ +1\sin\beta, & \ldots\ldots \end{cases}$$

Consequently,

$$\sin[\beta L(t)] \equiv L(t)\sin\beta\,. \tag{B.3}$$

Substitution of Equations B.2 and B.3 into Equation B.1 gives the desired expression:

$$E\cos[\omega_c t + \beta L(t)] = E[\cos\beta\cos\omega_c t - L(t)\sin\beta\sin\omega_c t]\,. \tag{B.4}$$

Spectrum of Signal

The Fourier series expansion for $L(t)$ is

$$\frac{4}{\pi}\sum_{N=1}^{\text{odd}}\frac{\sin N\omega_a t}{N}, \quad \omega_a = \frac{2\pi}{P}\,. \tag{B.5}$$

After substitution of this series into Equation B.4, the expression for a signal with square-wave PM is

$$E\cos[\omega_c t + \beta L(t)] = E\left[\cos\omega_c t\cos\beta - \left(\frac{4}{\pi}\sum_{N=1}^{\text{odd}}\frac{\sin N\omega_a t}{N}\right)\sin\beta\sin\omega_c t\right]\,. \tag{B.6}$$

With use of the identity $\sin A\sin B \equiv \frac{1}{2}\cos(A-B) - \frac{1}{2}\cos(A+B)$, Equation B.6 expands to give the desired spectrum as

$$E\cos\beta\cos\omega_c t + E(\sin\beta)\frac{2}{N\pi}\sum_{1=N}^{\text{odd}}\cos(\omega_c t + N\omega_a t) - E(\sin\beta)\frac{2}{N\pi}\sum_{N=1}^{\text{odd}}\cos(\omega_c t - N\omega_a t)\,. \tag{B.7}$$

carrier — upper sidebands — lower sidebands

Appendix C

Signal Expression and Spectrum of a PM Signal With Quadrature AM

Signal Expression

If a carrier is phase modulated by a square wave and simultaneously amplitude modulated with an identical square wave shifted in time by a quarter period, the signal can be written as

$$E[1 + ML(t + P/4)] \cos[\omega_c t + \beta L(t)] \ , \tag{C.1}$$

where

M = AM index ($0 \leqslant M \leqslant 1$),

β = PM index (radians),

P = period of $L(t)$.

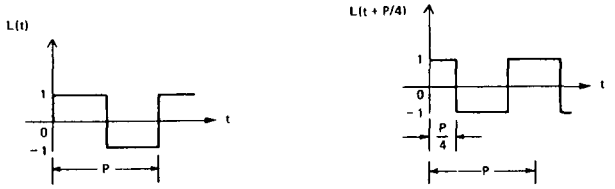

Equation C.1 expands as follows with use of the identity for $\cos(A+B)$ and Equation B.2 (Appendix B):

$$E[1 + ML(t + P/4)] [\cos\beta \cos\omega_c t - L(t) \sin\beta \sin\omega_c t] \ . \tag{C.2}$$

After multiplication by the AM factor, the signal expression consists of the sum of the following four terms (where $E = 1$ temporarily):

$$\cos\beta \cos\omega_c t \ , \tag{C.3}$$

$$-L(t) \sin\beta \sin\omega_c t \ , \tag{C.4}$$

$$L(t+P/4)M \cos\beta \cos\omega_c t, \tag{C.5}$$

$$-L(t + P/4)L(t)M \sin\beta \sin\omega_c t = -L(2t)M \sin\beta \sin\omega_c t \ . \tag{C.6}$$

In regard to Equation C.6, the equality

$$L(t + P/4)L(t) = L(2t)$$

is deduced from the diagram shown below Equation C.1; the factor $L(2t)$ is a unit-amplitude square wave with a period $P/2$.

Collecting the terms C.3 through C.6 gives the signal expression in terms of quadrature and in-phase components:

$$E[1 + ML(t + P/4)] \cos[\omega_c t + \beta L(t)]$$

$$= E \cos\beta \cos\omega_c t + EL(t + P/4)M \cos\beta \cos\omega_c t - E[L(t) + ML(2t)] \sin\beta \sin\omega_c t \,. \quad \text{(C.7)}$$

carrier | in-phase modulation | quadrature modulation

Spectrum of Signal

To derive the spectrum, we relist Equations C.3 through C.6 as below on the left and then list the equivalent for each of these terms on the right using the Fourier expansions for $L(t)$, $L(t + P/4)$, and $L(2t)$:

$$-L(t) \sin\beta \sin\omega_c t = -\sin\beta (\sin\omega_c t) \frac{4}{\pi} \sum_{N=1}^{\infty} \frac{\sin[(2N-1)\omega_a t]}{2N-1}, \quad \text{(C.8)}$$

$$L(t + P/4)M \cos\beta \cos\omega_c t = -M \cos\beta (\cos\omega_c t) \frac{4}{\pi} \sum_{N=1}^{\infty} \frac{(-1)^N \cos[(2N-1)\omega_a t]}{2N-1}, \quad \text{(C.9)}$$

$$-L(2t)M \sin\beta \sin\omega_c t = -M \sin\beta (\sin\omega_c t) \frac{4}{\pi} \sum_{N=1}^{\infty} \frac{\sin[(2N-1)2\omega_a t]}{2N-1}. \quad \text{(C.10)}$$

The equivalents on the right in Equations C.8 through C.10 are expanded with the identity

$$\cos(A + B) \equiv \cos A \cos B - \sin A \sin B \quad \text{or} \quad \sin A \sin B \equiv \tfrac{1}{2}\cos(A - B) - \tfrac{1}{2}\cos(A + B) :$$

Equation C.8 expands to

$$-\frac{2 \sin\beta}{\pi(2N-1)} \left\{ -\cos[\omega_c t + (2N-1)\omega_a t] + \cos[\omega_c t - (2N-1)\omega_a t] \right\}. \quad \text{(C.11)}$$

Equation C.9 expands to

$$-\frac{2M \cos\beta (-1)^N}{\pi(2N-1)} \left\{ \cos[\omega_c t + (2N-1)\omega_a t] + \cos[\omega_c t - (2N-1)\omega_a t] \right\}. \quad \text{(C.12)}$$

Equation C.10 expands to

$$-\frac{2M\sin\beta}{\pi(2N-1)}\left\{-\cos[\omega_c t+(2N-1)2\omega_a t]+\cos[\omega_c t-(2N-1)2\omega_a t]\right\}. \qquad \text{(C.13)}$$

In Equations C.11 through C.13, $N = 1, 2, 3, \ldots$. We add Equations C.11 and C.12 to obtain upper and lower sidebands of odd order in ω_a [with index $(2N-1)\omega_a$]; upper and lower sidebands with even order in ω_a [with index $(2N-1)2\omega_a$] are given directly by Equation 13. The spectrum tabulated below then results:

$$E[1+ML(t+P/4)]\cos[\omega_c t+\beta L(t)] = E\cos\beta\cos\omega_c t$$

(carrier)

$$+\frac{2E}{\pi(2N-1)}[\sin\beta - M(-1)^N\cos\beta]\cos[\omega_c t+(2N-1)\omega_a t]$$

(upper sidebands, *odd* order in ω_a)

$$-\frac{2E}{\pi(2N-1)}[\sin\beta + M(-1)^N\cos\beta]\cos[\omega_c t-(2N-1)\omega_a t]$$

(lower sidebands, *odd* order in ω_a)

$$+\frac{2EM\sin\beta}{\pi(2N-1)}\cos[\omega_c t+(2N-1)2\omega_a t]$$

(upper sidebands, *even* order in ω_a)

$$-\frac{2EM\sin\beta}{\pi(2N-1)}\cos[\omega_c t-(2N-1)2\omega_a t], \qquad \text{(C.14)}$$

(lower sidebands, *even* order in ω_a)

where $\omega_a = 2\pi/P$ and $N = 1, 2, 3, \ldots$.

Appendix D

Signal Expression, Spectrum, and Phasor Diagram of a PM Signal With In-Phase AM

Derivation of Signal Expression in Terms of Quadrature and In-Phase Components

The expression for a carrier simultaneously phase and amplitude modulated by a square wave $L(t)$ is

$$E[1 + ML(t)] \cos [\omega_c t + \beta L(t)] . \tag{D.1}$$

Equation D.1 expands as follows according to Equation B.4 (Appendix B):

$$E[1 + ML(t)][\cos\beta \cos \omega_c t - L(t) \sin\beta \sin \omega_c t] . \tag{D.2}$$

Multiplying by the first term in brackets gives

$$\cos\beta \cos \omega_c t - L(t) \sin\beta \sin \omega_c t + ML(t) \cos\beta \cos \omega_c t - ML^2(t) \sin\beta \sin \omega_c t . \tag{D.3}$$

In the last term above, $L^2(t) \equiv 1$. Substitution of this relationship into Equation D.3 gives the desired expression:

$$E[1 + ML(t)] \cos [\omega_c t + \beta L(t)]$$

$$= \underset{\substack{\text{in-phase} \\ \text{carrier} \\ \text{component}}}{\cos\beta \cos \omega_c t} \underset{\substack{\text{quadrature} \\ \text{carrier} \\ \text{component}}}{- M \sin\beta \sin \omega_c t} + \underset{\substack{\text{in-phase} \\ \text{modulation} \\ \text{component}}}{ML(t) \cos\beta \cos \omega_c t} \underset{\substack{\text{quadrature} \\ \text{modulation} \\ \text{component}}}{- L(t) \sin\beta \sin \omega_c t} . \tag{D.4}$$

Signal Phasor Diagram

To determine the phasor diagram, we first rewrite Equation D.4 in a more compact form:

$$E_{\text{signal}} = E \cos\beta \cos \omega_c t - EM \sin\beta \sin \omega_c t + I_M \cos \omega_c t - Q_M \sin \omega_c t , \tag{D.5}$$

where

$$I_M = EL(t)M \cos\beta$$

$$Q_M = EL(t) \sin\beta.$$

To convert this equation to phasor form, we choose $\cos \omega_c t$ as the reference phasor:

$$\cos \omega_c t = \mathrm{Re}\{\bar{v} e^{j\omega_c t}\} ,$$

where $\bar{v}$ is the unit-amplitude phasor lying on the real axis. Then, the term $-\sin \omega_c t$ (Equation D.5) will lie on the $+j$ axis because

$$\begin{aligned} -\sin \omega_c t &\equiv \cos\left(\omega_c t + \frac{\pi}{2}\right) \\ &= \mathrm{Re}\{\bar{v} e^{j\pi/2} e^{j\omega_c t}\} \\ &= \mathrm{Re}\{j\bar{v} e^{j\omega_c t}\} , \end{aligned}$$

since $e^{j\pi/2} = +j$. With $\cos \omega_c t$ as the reference phasor, Equation D.5 in phasor notation is

$$E_{\text{signal}} = E(\cos \beta)\bar{v} + jEM(\sin \beta)\bar{v} + I_M \bar{v} + jQ_M \bar{v} . \tag{D.6}$$

Part A of Figure D.1 shows the phasor diagram of this equation with carrier phasors shown as solid lines; modulation phasors Q_M and I_M are shown as dotted lines. Since Q_M and I_M contain the square wave $L(t)$, the phasors representing Q_M and I_M would periodically reverse direction; the direction as drawn corresponds to periods of time when $L(t)$ is positive.

The quadrature carrier phasor $EM \sin \beta$, shown in Part A, is particularly significant because when this component is added vectorially to form the resultant carrier, the resultant carrier is no longer colinear or in quadrature with respect to the original modulation phasors I_M and Q_M. The *resultant* carrier provides the phase reference when this signal is demodulated; consequently, it is necessary to determine a new set of colinear and quadrature modulation components relative to the resultant carrier. Parts B and C of Figure D.1 show the steps involved in this derivation. From Part A, the resultant carrier is displaced α degrees with respect to the real axis, $\alpha = \tan^{-1}(M \sin \beta / \cos \beta)$; consequently, the angle α is known immediately once the AM index M and PM index β are specified. For later use, from an inspection of Part A,

$$\begin{aligned} \sin \alpha &= \frac{M \sin \beta}{\sqrt{\cos^2 \beta + M^2 \sin^2 \beta}} \\ \cos \alpha &= \frac{\cos \beta}{\sqrt{\cos^2 \beta + M^2 \sin^2 \beta}} . \end{aligned} \tag{D.7}$$

In Part B, the phasor system has been rotated α degrees so as to make the resultant carrier the phase reference. A new modulation set is determined as follows: With respect to the resultant carrier, Q_M has a quadrature component

$$Q_M \sin (90 - \alpha) = Q_M \cos \alpha$$

while I_M has a quadrature component

$$I_M \sin (-\alpha) = -I_M \sin \alpha .$$

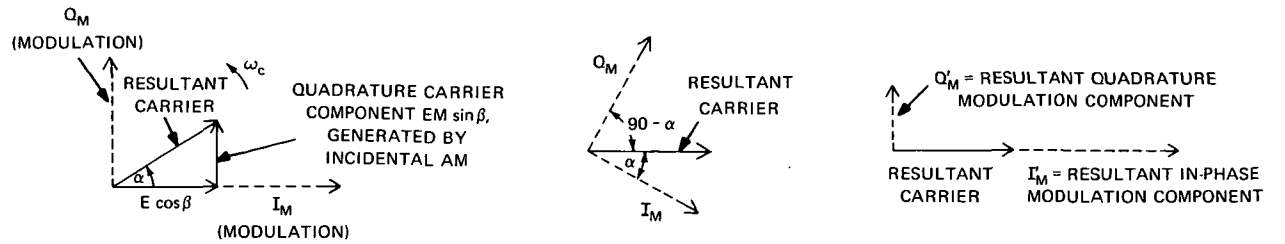

(A) Diagram with carrier component cos $\omega_c t$ as reference phasor.

(B) Diagram after rotation to make resultant carrier the reference phasor.

(C) Diagram showing resultant modulation components Q'_m and I'_m obtained by projection.

Figure D.1—Development of phasor diagram for in-phase AM.

The new quadrature phasor Q'_M with respect to the resultant carrier is the sum

$$Q'_M = Q_M \cos\alpha - I_M \sin\alpha . \tag{D.8}$$

The new in-phase phasor I'_M is given by the sum of the terms

$$I_M \cos(-\alpha) = I_M \cos\alpha \quad \text{and} \quad Q_M \cos(90 - \alpha) = Q_M \sin\alpha :$$

$$I'_M = I_M \cos\alpha + Q_M \sin\alpha . \tag{D.9}$$

To determine the amplitude of Q'_M in terms of the original phasor Q_M and I_M, we substitute their definition from Equation D.5 and the equivalents for $\cos\alpha$ and $\sin\alpha$ from Equation D.7 into Equation D.8:

$$Q'_M = L(t)\frac{(\sin\beta)(1-M^2)E}{\sqrt{1 + M^2 \tan^2\beta}} . \tag{D.10}$$

The amplitude of I'_M is obtained by substituting Q_M and I_M from Equation D.5 and $\cos\alpha$ and $\sin\alpha$ from Equation D.7 into Equation D.9:

$$I'_M = \frac{L(t)ME}{\cos\beta\sqrt{1 + M^2 \tan^2\beta}} . \tag{D.11}$$

Finally, given Q'_M and I'_M as above, the phasor diagram shown in Part C of Figure C.1, can be reconverted to give an equivalent expression in terms of $\cos\omega_c t$ and $\sin\omega_c t$:

$$E_{\text{signal}} = E\sqrt{\cos^2\beta + M^2 \sin^2\beta}\cos\omega_c t + \frac{EML(t)}{\cos\beta\sqrt{1 + M^2 \tan^2\beta}}\cos\omega_c t$$

$$- \frac{E(\sin\beta)(1-M^2)}{\sqrt{1 + M^2 \tan^2\beta}} L(t) \sin\omega_c t . \tag{D.12}$$

Spectrum

To determine the spectrum, first, we rewrite Equation D.4 as follows:

$$E_{\text{signal}} = \underset{\text{carrier}}{E(\cos\beta \cos\omega_c t - M \sin\beta \sin\omega_c t)} + \underset{\text{modulation}}{EL(t)(M \cos\beta \cos\omega_c t - \sin\beta \sin\omega_c t)} . \quad \text{(D.13)}$$

The carrier and modulation terms consist of a sum involving $\cos\omega_c t$ and $\sin\omega_c t$ which can be combined into single terms in ω_c according to the identity

$$A \cos\alpha - B \sin\alpha \equiv R \cos(\alpha + \phi) ,$$

where $R = (A^2 + B^2)^{1/2}$ and $\phi = \tan^{-1}(B/A)$; then,

$$E_{\text{signal}} = E(\cos^2\beta + M^2 \sin^2\beta)^{1/2} \cos\left\{\omega_c t + \tan^{-1}[(M \sin\beta)/\cos\beta]\right\}$$

$$+ EL(t)(M^2 \cos^2\beta + \sin^2\beta)^{1/2} \cos\left\{\omega_c t - \tan^{-1}[(\sin\beta)/M \cos\beta]\right\} . \quad \text{(D.14)}$$

The first term is the carrier, while the second term represents the modulation; this later term accounts for the sideband structure of the spectrum, which can be derived as follows: First, we expand $L(t)$ in a Fourier series:

$$L(t) = \frac{4}{\pi} \sum_{N=1}^{\text{odd}} \frac{\sin N\omega_a t}{N} ,$$

where $\omega_a = 2\pi/P$ (P = period of $L(t)$). Then, we compute the product

$$\frac{4}{\pi} \sum_{N=1}^{\text{odd}} \sin\frac{N\omega_a t}{N} \cos\left\{\omega_c t - \tan^{-1}[(\sin\beta)/M \cos\beta]\right\}$$

$$= \frac{2}{N\pi} \sin\left\{\omega_c t + N\omega_a t - \tan^{-1}[(\sin\beta)/M \cos\beta]\right\}$$

$$- \sin\left\{\omega_c t - N\omega_a t - \tan^{-1}[(\sin\beta)/M \cos\beta]\right\} , \quad N = 1, 3, 5, \ldots \quad \text{(D.15)}$$

according to the identity

$$\sin A \cos B = \tfrac{1}{2}[\sin(B + A) - \sin(B - A)] .$$

In taking this product, the amplitude factor $(M^2 \cos^2 \beta + \sin^2 \beta)^{1/2}$ has been temporarily omitted. With this factor restored and noting that the carrier is the first term of Equation D.14, the spectrum can then be listed as follows:

$$\text{Carrier} = E(\cos^2 \beta + M^2 \sin^2 \beta)^{1/2} \cos [\omega_c t + \tan^{-1} (M \tan \beta)] ,$$

$$\text{Upper sidebands } (N = 1, 3, \ldots) = \frac{2E}{N\pi} (M^2 \cos^2 \beta + \sin^2 \beta)^{1/2} \sin \left\{ \omega_c t + N\omega_a t - \tan^{-1} [(\tan \beta)/M] \right\} ,$$

$$\text{Lower sidebands } (N = 1, 3, \ldots) = -\frac{2E}{N\pi} (M^2 \cos^2 \beta + \sin^2 \beta)^{1/2} \sin \left\{ \omega_c t - N\omega_a t - \tan^{-1} [(\tan \beta)/M] \right\} .$$

NATIONAL AERONAUTICS AND SPACE ADMISTRATION
WASHINGTON, D.C. 20546

OFFICIAL BUSINESS
PENALTY FOR PRIVATE USE $300

FIRST CLASS MAIL

POSTAGE AND FEES PAID
NATIONAL AERONAUTICS AND
SPACE ADMINISTRATION

U.S.MAIL

POSTMASTER: If Undeliverable (Section 158 Postal Manual) Do Not Return

"The aeronautical and space activities of the United States shall be conducted so as to contribute . . . to the expansion of human knowledge of phenomena in the atmosphere and space. The Administration shall provide for the widest practicable and appropriate dissemination of information concerning its activities and the results thereof."

—NATIONAL AERONAUTICS AND SPACE ACT OF 1958

NASA SCIENTIFIC AND TECHNICAL PUBLICATIONS

TECHNICAL REPORTS: Scientific and technical information considered important, complete, and a lasting contribution to existing knowledge.

TECHNICAL NOTES: Information less broad in scope but nevertheless of importance as a contribution to existing knowledge.

TECHNICAL MEMORANDUMS: Information receiving limited distribution because of preliminary data, security classification, or other reasons.

CONTRACTOR REPORTS: Scientific and technical information generated under a NASA contract or grant and considered an important contribution to existing knowledge.

TECHNICAL TRANSLATIONS: Information published in a foreign language considered to merit NASA distribution in English.

SPECIAL PUBLICATIONS: Information derived from or of value to NASA activities. Publications include conference proceedings, monographs, data compilations, handbooks, sourcebooks, and special bibliographies.

TECHNOLOGY UTILIZATION PUBLICATIONS: Information on technology used by NASA that may be of particular interest in commercial and other non-aerospace applications. Publications include Tech Briefs, Technology Utilization Reports and Technology Surveys.

Details on the availability of these publications may be obtained from:

SCIENTIFIC AND TECHNICAL INFORMATION OFFICE

NATIONAL AERONAUTICS AND SPACE ADMINISTRATION

Washington, D.C. 20546